JOINT TRANSPORTATION
RESEARCH PROGRAM
INDIANA DEPARTMENT OF TRANSPORTATION
AND PURDUE UNIVERSITY

A Laboratory Study of Apron-Riprap Design for Small-Culvert Outlets

High-tailwater case

Low-tailwater case

**Dennis A. Lyn, Siddharth Saksena,
Sayan Dey, Venkatesh Merwade**

SPR-3916 • Report Number: FHWA/IN/JTRP-2019/16 • DOI: 10.5703/1288284316975

RECOMMENDED CITATION

Lyn, D. A., Saksena, S., Dey, S., & Merwade, V. (2019). *A laboratory study of apron-riprap design for small-culvert outlets* (Joint Transportation Research Program Publication No. FHWA/IN/JTRP-2019/16). West Lafayette, IN: Purdue University. https://doi.org/10.5703/1288284316975

AUTHORS

Dennis A. Lyn, PhD
Professor of Civil Engineering
Lyles School of Civil Engineering
Purdue University
lyn@purdue.edu
(765) 494-9615
Corresponding Author

Siddharth Saksena
Sayan Dey
Graduate Research Assistants
Lyles School of Civil Engineering
Purdue University

Venkatesh Merwade, PhD
Professor of Civil Engineering
Lyles School of Civil Engineering
Purdue University
vmerwade@purdue.edu
(765) 494-2176
Corresponding Author

JOINT TRANSPORTATION RESEARCH PROGRAM

The Joint Transportation Research Program serves as a vehicle for INDOT collaboration with higher education institutions and industry in Indiana to facilitate innovation that results in continuous improvement in the planning, design, construction, operation, management and economic efficiency of the Indiana transportation infrastructure. https://engineering.purdue.edu/JTRP/index_html

Published reports of the Joint Transportation Research Program are available at http://docs.lib.purdue.edu/jtrp/.

NOTICE

TECHNICAL REPORT DOCUMENTATION PAGE

1. Report No. FHWA/IN/JTRP-2019/16	2. Government Accession No.	3. Recipient's Catalog No.
4. Title and Subtitle A Laboratory Study of Apron-Riprap Design for Small-Culvert Outlets		**5. Report Date** July 2019 **6. Performing Organization Code**
7. Author(s) Dennis A. Lyn, Siddharth Saksena, Sayan Dey, Venkatesh Merwade		**8. Performing Organization Report No.** FHWA/IN/JTRP-2019/16
9. Performing Organization Name and Address Joint Transportation Research Program Hall for Discovery and Learning Research (DLR), Suite 204 207 S. Martin Jischke Drive West Lafayette, IN 47907		**10. Work Unit No.** **11. Contract or Grant No.** SPR-3916
12. Sponsoring Agency Name and Address Indiana Department of Transportation (SPR) State Office Building 100 North Senate Avenue Indianapolis, IN 46204		**13. Type of Report and Period Covered** Final Report **14. Sponsoring Agency Code**

15. Supplementary Notes

Conducted in cooperation with the U.S. Department of Transportation, Federal Highway Administration.

16. Abstract

The present study investigated primarily the appropriate stone-sizing of on-grade riprap aprons, and more specifically whether the current INDOT design policy may be overly conservative especially within the context of smaller culverts. In the study, laboratory experiments were performed with two pipe diameters, D = 4.25 in (0.35 ft) and 5.75 in (0.48 ft), and four stone sizes, median diameters estimated to be d_{50} = 0.61 in, 1.22 in, 1.73 in, and 2.24 in, for a range of discharges and tailwater depths. Video records were made of the laboratory apron to detect stone-mobilization events, and stable and unstable cases were distinguished. Logistic regression was then applied to develop equations delineating the boundary between stable and unstable regions for different riprap size classes in terms of d_{50}/D. These regression equations were then modified to ensure that they formed an ordered system in that each equation was more conservative than the next, to include a safety factor, and to set a minimum size for each size class consistent with the applicability of each equation. Procedures for applying the proposed equations are described.

Compared to the current INDOT design policy, the proposed approach typically predicts a smaller standard riprap class required for apron stability. In an application to a sample of actual culverts, the proposed approach, including the recommended safety factors, yielded a smaller required standard INDOT riprap class in 75% of cases, but, in a small number of cases with very low relative tailwater depths, did recommend a more conservative design. Of the other two main approaches to stone sizing for riprap aprons, the HEC-14 model was rather restricted in its range of application, but where applicable it was found to be somewhat more conservative in its stone-size recommendation, though in practice the recommended riprap class largely agreed with the proposed approach. The results of the other main approach, that due to Bohan (1970), were more erratic, with the maximum-tailwater equation being too lax and the minimum-tailwater equation being generally too stringent. Both the HEC-14 and the Bohan models tended to be less conservative than the proposed approach for larger values of d_{50}/D.

A secondary aim of the study was an examination of the velocity field downstream of the outlet, and the possible implications for scour downstream of the apron. Point velocity measurements were obtained for four cases, all with the same 4.25-in diameter pipe, three of which involved the largest (d_{50} = 2.2 in) stone, and one over a smooth bed. In the three cases with a stone apron, the apron extended a distance of ≈ 9D downstream of the outlet. In all four cases, substantial velocities (maximum velociites greater than 70% of than the average outlet velocity) were observed beyond 4D (which is the minimum specified by INDOT design guidelines) and even beyond 8D (which is the largest apron length specified in HEC-14). A comparison between rough-bed and smooth-bed results indicated a measurable effect on maximum velocity due to the rough apron, but the reduction in maximum velocity is still likely insufficient to prevent scour downstream of the apron in most practical cases even if the apron extends to 9D.

17. Key Words	18. Distribution Statement
culvert, outlet protection, riprap, apron, stone sizing, velocity field	No restrictions. This document is available through the National Technical Information Service, Springfield, VA 22161.

19. Security Classif. (of this report)	20. Security Classif. (of this page)	21. No. of Pages	22. Price
Unclassified	Unclassified	40 including appendices	

EXECUTIVE SUMMARY

A LABORATORY STUDY OF APRON-RIPRAP DESIGN FOR SMALL-CULVERT OUTLETS

Introduction

The present study investigated primarily the appropriate stone sizing of on-grade riprap aprons, and more specifically whether the current INDOT design policy may be overly conservative, especially within the context of smaller culverts. In the study, laboratory experiments were performed with two pipe diameters, D=4.25 in (0.35 ft) and 5.75 in (0.48 ft), and four stone sizes—median diameters estimated to be d_{50}=0.61 in, 1.22 in, 1.73 in, and 2.24 in—for a range of discharges and tailwater depths. Video records were made of the laboratory apron to detect stone-mobilization events, and stable and unstable cases were distinguished. Logistic regression was then applied to develop equations delineating the boundary between stable and unstable regions for different riprap size classes in terms of d_{50}/D. These regression equations were then modified to ensure that they formed an ordered system in that each equation was more conservative than the next, to include a safety factor, and to set a minimum size for each size class consistent with the applicability of each equation. Procedures for applying the proposed equations are described.

Findings

Compared to the current INDOT design policy, the proposed approach typically predicts a smaller standard riprap class required for apron stability. In an application to a sample of actual culverts, the proposed approach, including the recommended safety factors, yielded a smaller required standard INDOT riprap class in 75% of cases, but, in a small number of cases with very low relative tailwater depths, the proposed approach did recommend a more conservative design. Of the other two main approaches to stone sizing for riprap aprons, the HEC-14 model was rather restricted in its range of application, but where applicable it was found to be somewhat more conservative in its stone-size recommendation, though in practice the recommended riprap class largely agreed with the proposed approach. The results of the other main approach, that due to Bohan (1970), were more erratic, with the maximum-tailwater equation being too lax and the minimum-tailwater equation being generally too stringent. Both the HEC-14 and the Bohan models tended to be less conservative than the proposed approach for larger values of d_{50}/D.

A secondary aim of the study was an examination of the velocity field downstream of the outlet, and the possible implications for scour downstream of the apron. Point velocity measurements were obtained for four cases, all with the same 4.25-in diameter pipe, three of which involved the largest (d_{50}=2.2 in) stone, and one over a smooth bed. In the three cases with a stone apron, the apron extended a distance of $\approx 9D$ downstream of the outlet. In all four cases, substantial velocities (maximum velocities greater than 70% of the average outlet velocity) were observed beyond $4D$ (which is the minimum specified by INDOT design guidelines) and even beyond $8D$ (which is the largest apron length specified in HEC-14). A comparison between rough-bed and smooth-bed results indicated a measurable effect on maximum velocity due to the rough apron, but the reduction in maximum velocity is still likely insufficient to prevent scour downstream of the apron in most practical cases, even if the apron extends to $9D$.

CONTENTS

TABLES

FIGURES

1. INTRODUCTION, PROBLEM STATEMENT, AND SCOPE

Traditional culvert hydraulic design typically results, under design conditions, in the flow area within the culvert being significantly reduced from the original stream cross-sectional area, and hence with an outlet velocity capable of causing substantial streambed erosion in the vicinity of the outlet. Consequently, some scour protection is usually required at outlets (and at inlets). According to Thompson and Kilgore (2006, to be referred to below as HEC-14), the most common outlet protection, especially for smaller culverts (less than 1500 mm or 5 ft in diameter), is the simple riprap apron. This scour-protection measure consists of one or more layers of stone on grade, extending for some distance downstream of the culvert outlet, and intended to act as armor for the much more erodible streambed substrate. Figure 1.1 (taken from HEC-14) shows two common apron configurations at a culvert outlet.

Several design questions arise in connection with riprap aprons, the foremost being the choice of stone size or riprap class for any given design condition. Current Indiana Department of Transportation (INDOT) guidelines make no distinction between riprap sizing for streambank protection or for culvert outlets, applying the same design procedure to both situations. This procedure considers only the velocity, v, (in the culvert outlet problem, only the averaged outlet velocity, typically estimated using the standard software, HY-8) in the choice of stone size. The design guidance is summarized in Table 1.1, where INDOT standard specifications assume only three standard riprap classes (revetment, and classes 1 and 2), with gradations as defined in Table 1.2.

The INDOT Hydraulics Group raised questions regarding whether the current INDOT design procedure based solely on velocities may be overly conservative, particularly in the context of smaller culverts. A specific case, discussed in more detail in Appendix A, is illustrative. A hydraulic analysis of the performance of a circular culvert of diameter 4 ft performed using HY-8 found an outlet velocity of 12.4 ft/s. The recommended riprap, following the current INDOT design policy, would be class 2 riprap because the outlet velocity lies between 10 ft/s and 13 ft/s. This is relatively large material that would incur additional construction costs, motivating the question whether a smaller riprap class would provide adequate protection for the specified design conditions.

While the present study focuses on the issue of stone sizing, riprap-apron design also must deal with the apron geometry (length and width). The present study does address the latter issue in a limited manner by examining the downstream development of the transverse velocity profile, thereby delineating the downstream region where high velocities capable of scouring the bed might be expected. More specifically, the extent to which a very rough riprap apron might dissipate the outlet flow energy was of interest.

The report is organized as follows. Chapter 2 reviews the major existing alternative riprap-apron design approaches, and introduces a new framework for comparing different approaches and for developing a new approach. Chapter 3 discusses the experimental aspects of the study, including measurements and instrumentation,

TABLE 1.1
INDOT riprap design guidelines

Erosion-Protection Method	Velocity, v (ft/s)
Revetment Riprap	≤ 6.5
Class 1 Riprap	$6.5 < v < 10$
Class 2 Riprap	$10 \leq v \leq 13$
Energy Dissipator	>13

Source: INDOT Hydraulics and Drainage Design manual, Chap. 203, Figure 203-2D9 (INDOT, 2017).

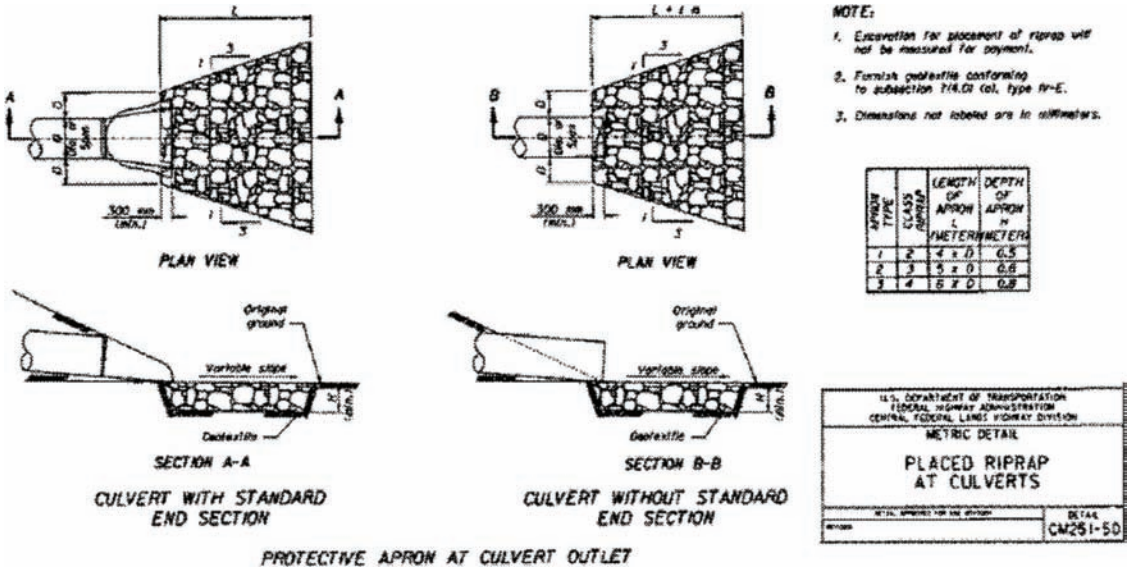

Figure 1.1 Plan and profile views of two types of riprap aprons (taken from HEC-14).

TABLE 1.2
INDOT standard riprap gradation and size

GRADATION REQUIREMENTS					
	Percent Smaller				
Size (in)	Revetment (%)	Class 1 (%)	Class 2 (%)	Uniform A (%)	Uniform B (%)
30			100		
24		100	85–100		
18	100	85–100	60–80		
12	90–100	35–50	20–40		
8				100	
6	20–40	10–30	0–20	35–80	95–100
3	0–10	0–10	0–10		35–80
1				0–20	0–20
Depth of Riprap, minimum	18 in	24 in	30 in		

Source: INDOT Standard Specifications, Section 904.04 9 (INDOT, 2018).

Note: In the following, it is assumed that the median diameter, d_{50}, for the standard INDOT riprap classes are: for revetment class, d_{50}=7 in= 0.58 ft; for class 1, d_{50}=12 in=1 ft; and for class 2, d_{50}=15 in=1.25 ft.

as well as the basic data analysis to be undertaken. The experimental results together with proposed stone-sizing equations and procedure are presented in Chapter 4, which also includes an application to a sample of actual culverts. A summary of the study is given in Chapter 5, which also gives design recommendations.

2. ALTERNATIVE APRON DESIGN EQUATIONS

In this chapter, apron design equations specifically for culvert outlets are discussed, emphasizing the choice of stone size. A definition sketch with the important variables defined is given in Figure 2.1.

Two approaches to riprap-apron design are examined in detail, namely that proposed by Bohan (1970) and that by Fletcher and Grace (1972). Developed for the U.S. Army Corps of Engineers, both have been adopted by a number of state agencies in some form, with that of Fletcher and Grace (1972) being recommended in HEC-14 for culvert-outlet aprons. Appendix D of HEC-14 reviews several of the stone-sizing equations to be discussed, and includes a comparison of their predictions for specific numerical cases. A generic equation, more associated with riprap for streambank protection, is also discussed, as it has a solid theoretical as well as empirical foundations, and hence may provide the basis for a proposed synthesis or framework equation. Although it may seem unusual to include a streambank equation in this discussion of culverts, the current INDOT guidelines do not distinguish between streambank and culvert applications. The framework stone-sizing equation permits convenient comparison of different approaches and also forms the basis of proposed equations to be developed.

2.1 The Bohan Equations (1970)

The main experimental study on stone sizing for culvert-outlet aprons is that of Bohan (1970), who also proposed one of the models still widely used today. A key observation of that study is the distinctly different scour behavior depending on the tailwater level. Bohan (1970) argued that his experimental results could be grouped into two categories, namely a minimum-tailwater condition, and a maximum-tailwater condition, with the distinction being operationally defined in terms of the ratio of tailwater level to culvert diameter, t_w/D (his study was largely restricted to circular-pipe culverts). As such, his model equation is specified for each category:

$$\frac{d_{50}}{D} = 0.25 Fr_{D,out} = 0.25\left(\frac{V_{out}}{\sqrt{gD}}\right), \quad \frac{t_w}{D} \le \frac{1}{2}\begin{pmatrix}\text{minimum}\\ \text{tailwater condition}\end{pmatrix}$$
$$= 0.25 Fr_{D,out} - 0.15, \quad \frac{1}{2} < \frac{t_w}{D}\begin{pmatrix}\text{maximum}\\ \text{tailwater condition}\end{pmatrix} \qquad \text{(Eq. 2.1)}$$

where $Fr_{D,out}$ is the outlet Froude number, based on V_{out} the average flow velocity at the culvert outlet, and g is the acceleration due to gravity. Bohan (1970) did not specify d_{50}, but simply stated that uniformly graded stones were used in the experiment, but d_{50} is used here for consistency with the other equations to be discussed. While Bohan (1970) may not be specifically credited, the Bohan model (or a close variant) is often encountered in a simplified tabular or graphical form (e.g., Figure 2.2 from NRCS, 2004), the signature distinction between a minimum and a maximum tailwater condition clearly linking these forms to Equation 2.1. These forms are easier to use, but they often oversimplify Equation 2.1 in that full-flow velocities are used rather than outlet velocities, possibly leading to undersized stones. A potential problem with the high-tailwater equation is that it may yield negative values for the range $Fr_{D,out}$<0.6. This arose in an application to an actual INDOT culvert (see Chapter 4.4.3).

Two features of Equation 2.1 may be highlighted. Firstly, in contrast to the current INDOT design guidelines, the appropriate stone size depends not only on the

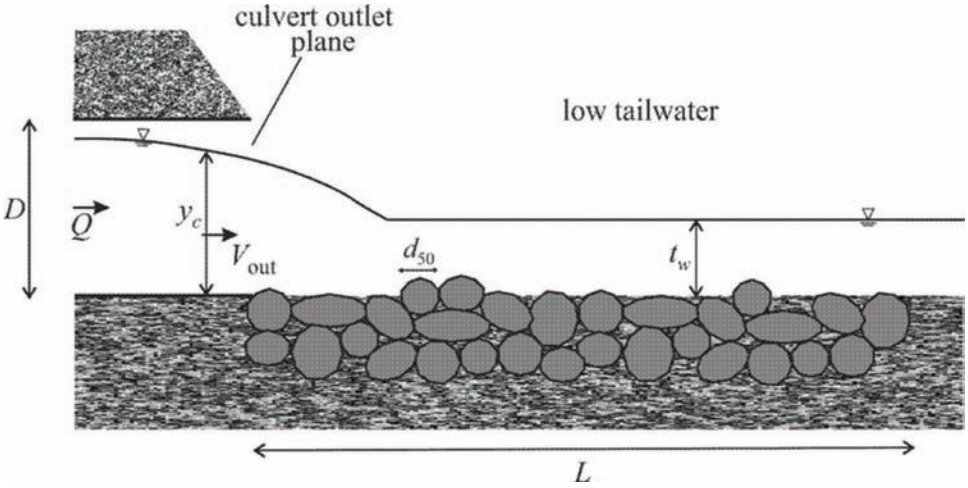

Figure 2.1 Definition sketch for culvert outlet and riprap apron.

outlet velocity, V_{out}, but also on the culvert size (D) and the tailwater depth, t_w. Secondly, the stone size required for stability under the maximum-tailwater condition may be significantly smaller than that required under the minimum tailwater condition. This opens up the possibility that, if tailwater (and perhaps culvert size) effects are explicitly incorporated in choosing stone size, then this may lead to smaller minimum riprap being found adequate, and allowing a more economical design compared to that complying with the current INDOT design, especially if higher tailwater levels are more likely to occur for small-culvert applications.

Bohan (1970) also provided a specification for the length, L_a, of the apron. In this, he distinguished not only between a minimum and a maximum tailwater, but also between cases with $Fr_{D,out}$ less than or greater than unity. Thus, his equation for L_a may be expressed as

$$\begin{aligned} L_a/D &= 8,\ Fr_{D,out} \le 1 \\ &= 8 + 17\log_{10} Fr_{D,out},\ Fr_{D,out} > 1 \text{ and } t_w/D < 1/2 \\ &= 8 + 55\log_{10} Fr_{D,out},\ Fr_{D,out} > 1 \text{ and } t_w/D \ge 1/2. \end{aligned} \quad \text{(Eq. 2.2)}$$

From Equation 2.2, the required L_a for maximum-tailwater (and $Fr_{D,out}>1$) conditions would be significantly larger than for the corresponding minimum-tailwater case. Hence, Equation 2.2 can lead to quite long aprons, with L_a/D exceeding 20 in extreme cases for maximum-tailwater conditions. Figure 2.2 also gives L_a though seems to make the additional assumption that $Fr_{D,out}>1$, thus using only the last two equations of Equation 2.2, possibly to compensate for a full-flow estimate of V_{out}. For comparison, the HEC-14 guidance for L_a varies with required stone size, d_{50} (Table 2.1), with a maximum L_a of $8D$, and does *not* include any dependence on tailwater conditions.

The INDOT guidelines for apron length are even simpler and less conservative, as it specifies a minimum L_a of only $4D$, independent of d_{50} and tailwater. Practical constraints on L_a, such as right-of-way considerations, point to the possibility that apron dimensions rather than stone size may be the limiting factor in apron scour design.

A specification for the lateral extent of the apron was also given by Bohan (1970) and as might be expected depends on the tailwater. Bohan (1970) observed that "The jet from the culvert dispersed rapidly with minimum tailwater, and required a short wide blanket; however, with maximum tailwater, the jet traveled a considerable distance downstream and required a long narrow blanket to prevent erosion." Thus a flare or expansion ratio of 1:2, i.e., one unit in the lateral direction to two units in the streamwise direction, was recommended for minimum-tailwater conditions, while a much narrower more elongated ratio of 1:5 was recommended for maximum-tailwater conditions (Figure 2.3). Not surprisingly, the same ratios are also found in Figure 2.2, but the apron width of Bohan (1970) at any streamwise section is larger by $2D$ than that in Figure 2.2 because the initial width at the culvert outlet is larger by the same amount. For comparison, the HEC-14 guidance recommends an intermediate ratio of 1:3, while the INDOT design manual specifies a ratio of 1:4, both without any regard to tailwater or other conditions.

The experimental basis for Bohan's recommended apron geometry should however be noted. The results were obtained with surrounding substrate the same for all experiments, namely a fine sand with a median diameter of $\approx$ 0.15 mm. Even when scaled to field conditions, this could still imply a medium sand substrate in the stream, which for some parameter range might be an overly conservative assumption.

2.2 The HEC-14 Equations (Fletcher and Grace, 1972)

The Bohan equations are based on the outlet Froude number, which require an estimate of the outlet velocity (V_{out}). This in the 1970's was not straightforward to obtain (as evidenced by the approximations necessary for Figure 2.2), and Fletcher and Grace (1972) was

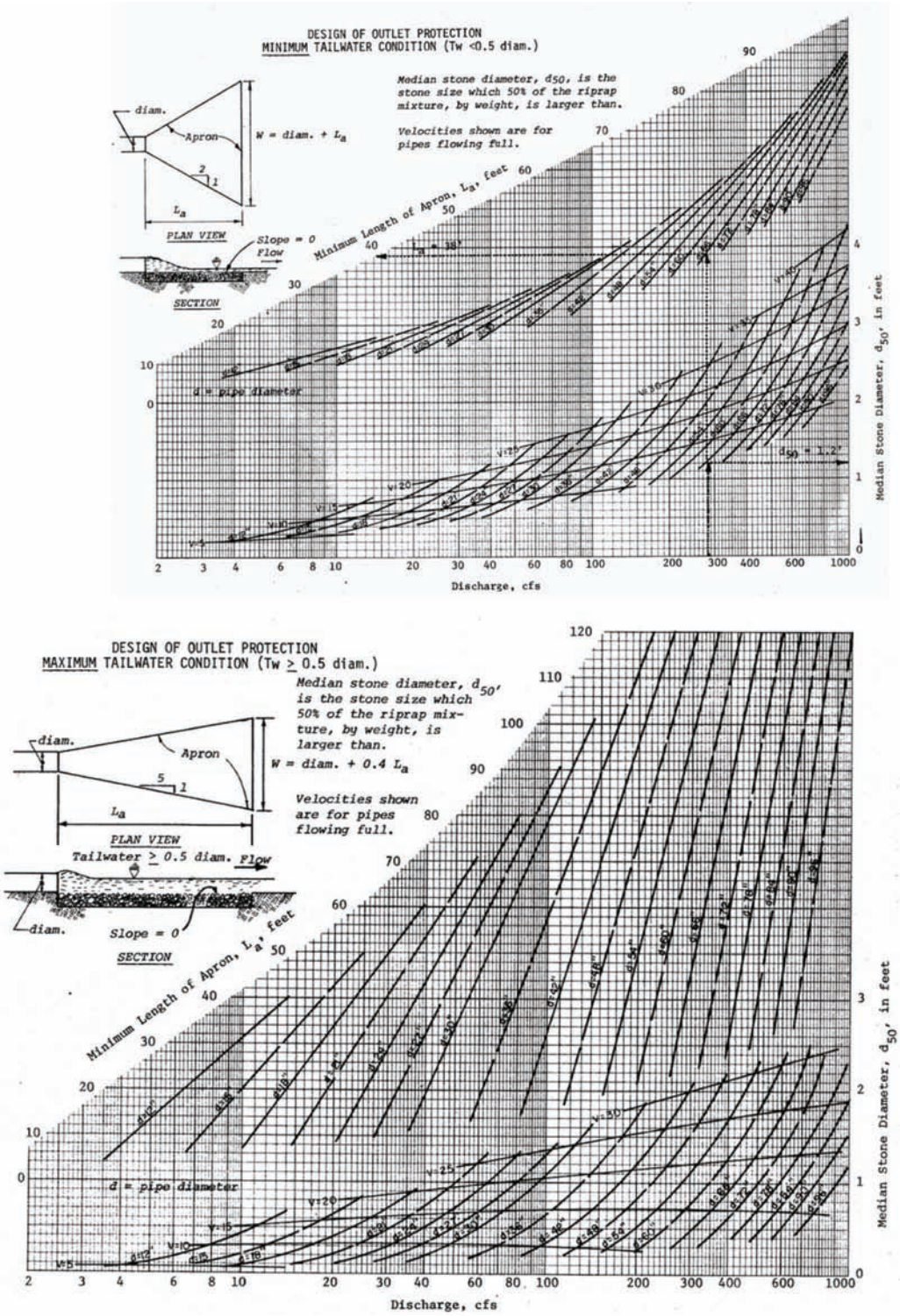

Figure 2.2 Simplified graphical form of the Bohan model for stone sizing and length of riprap aprons (e.g., from NRCS, 2004).

motivated to develop design equations involving more directly available variables, such as discharge, Q. Their stone-sizing equation may be expressed as

$$\frac{d_{50}}{D} = 0.2\left(\frac{Q}{\sqrt{gD^5}}\right)^{4/3}\left(\frac{D}{t_w}\right), \qquad \text{(Eq. 2.3)}$$

involving the same basic variables (D and t_w, but preferring the more available Q rather than V_{out}) as the Bohan model. Fletcher and Grace (1972) stated that this equation was based on the experimental results "reported by Bohan and subsequent unreported tests," and hence some degree of consistency between the two models should be expected. Equation 2.3 does differ

TABLE 2.1
HEC-14 guidance for the length and depth of a riprap apron as a function of required stone size

Required Stone Size, d_{50} (in)	Apron Length, L_a	Apron Depth
6	$4D$	3.3 d_{50}
10	$5D$	2.4 d_{50}
14	$6D$	2.2 d_{50}
20	$7D$	2.0 d_{50}
22	$8D$	2.0 d_{50}

notably from the Bohan model in that d_{50}/D is viewed as varying *continuously* with tailwater (t_w/D), whereas in the Bohan model, a more abrupt step variation with t_w/D (step change at $t_w/D=0.5$) is prescribed. This seems to have been the main reason for its adoption by HEC-14, which however restricts its range of application to $0.4 \leq t_w/D \leq 1$, and subcritical upstream flow (for supercritical culvert flows, a modified effective culvert diameter is recommended for use instead of the actual diameter). It also notes the implicit assumption of the standard stone specific gravity, $s=2.65$. In the following, Equation 2.3 will be applied following the HEC-14 restrictions and so will be termed the HEC-14 model.

The relationship to the Bohan model is more evident by the equation that Fletcher and Grace (1972) gave for the apron length:

$$\frac{L_a}{D} = 8 + 9.65\left(\frac{Q}{\sqrt{gD^5}}\right) \qquad \text{(Eq. 2.4)}$$

which like the corresponding Bohan model (Equation 2.2) gives as the minimum apron length, $(L_a)_{\min}=8D$. While Equation 2.4 does not explicitly make the distinction between minimum- and maximum-tailwater as in the Bohan model, in their prescription for the lateral extent of the apron, Fletcher and Grace (1972) did make the distinction, such that the apron geometry of both Bohan and of Fletcher and Grace are identical except for the use of Equation 2.4 rather than Equation 2.2. Despite its adoption of Equation 2.3, HEC-14 does *not* adopt Equation 2.4 but, as seen above in Table 2.1, gives a tabulated prescription that does not explicitly depend on either Q or t_w, depending only on stone size (which does vary with Q and t_w).

A dimensional version of Equation 2.3 is recommended in U.S. Department of Agriculture, Soil Conservation Service (1989), with a possibly slightly different constant coefficient, and also with more different prescriptions for the apron length. Similarly, a close variant of Equation 2.3 is adopted for circular culverts in the Urban Stormwater Drainage Criteria Manual (Urban Drainage and Flood Control District, 2017; hereafter referred to as the USDCM model), namely,

$$\frac{d_{50}}{D} = 0.13\left(\frac{Q}{\sqrt{gD^5}}\right)\left(\frac{D}{t_w}\right)^{1.2} \qquad \text{(Eq. 2.5)}$$

involving changes in both exponents as well as the constant coefficient.

2.3 Other Stone-Sizing Equations

The INDOT design practice where the stone size depends only on the outlet velocity may be viewed as

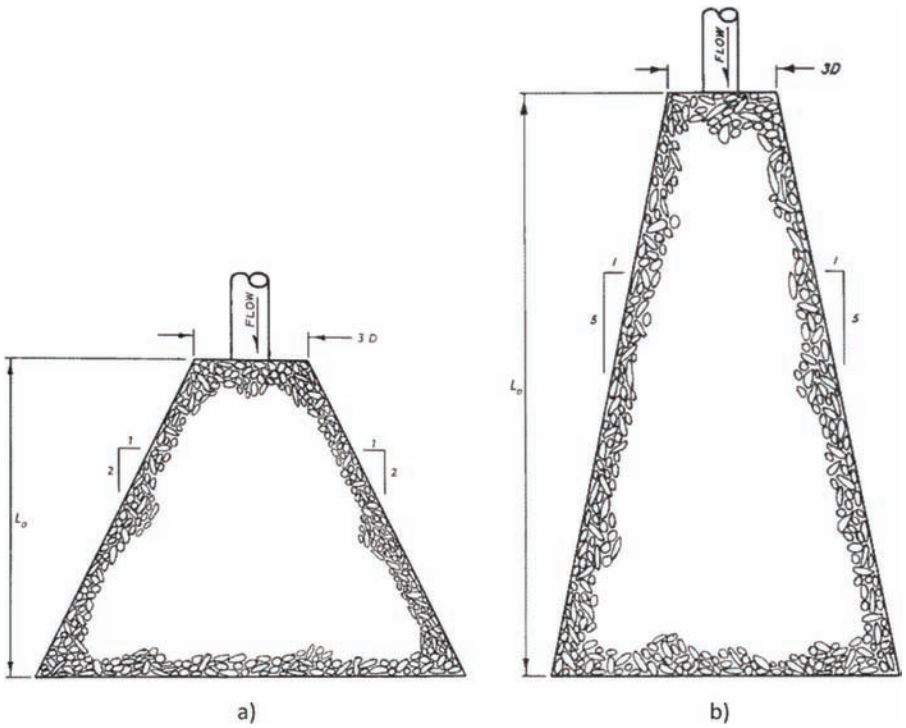

Figure 2.3 Apron geometry recommended in Bohan (1970) for (a) minimum- and (b) maximum-tailwater conditions.

being rooted in the early model of Berry (1948) and Peterka (1978) in which

$$d_{50} = \alpha V^2, \qquad \text{(Eq. 2.6)}$$

where α is a dimensional constant depending on the system of units (0.0126 for US customary units). Equation 2.6 yields values of d_{50} notably larger than that consistent with the INDOT practice; for example, $V=13$ ft/s is the INDOT limit for class 2 riprap ($d_{50} \approx 1.25$ ft), whereas Equation 2.6 prescribes $d_{50}=2.1$ ft. In its review, HEC-14 Appendix D also mentions the formulae of Searcy (1967), originally intended for application to pier protection but also used for riprap apron downstream of an energy dissipator, which is of the form

$$\frac{V^2}{g(s-1)d_{50}} = K, \qquad \text{(Eq. 2.7)}$$

where $K=2.89$. An equation of the same form is also associated with Isbash (1936), with a value of K chosen to range from 1.5 to 2.9, depending on turbulence level. Maynord, Ruff, and Abt (1989) comment that the Isbash equation is more appropriate in the absence of boundary layer development, which could be argued as characterizing better the culvert-outlet flow. The INDOT design practice would lead to values of K in the range between 1.3 and 2.6 (note that smaller values of K lead to larger values of d_{50}, and hence may be considered more conservative).

The simpler problem of the initiation of particle motion by an overlying uniform channel flow has been intensively studied, and so a solid theoretical and empirical foundation for riprap sizing under these restrictive conditions have been developed. Combining the classic Shields criterion for incipient sediment motion with a Manning-Strickler-type flow resistance model leads to a generic equation form (or "basic form" in the terminology of Lagasse, Clopper, Zevenbergen, and Ruff (2006), to be referred to as NCHRP-568) for stone sizing:

$$\frac{V^2}{g(s-1)d_{50}} = f\left(\frac{y}{d_{50}}\right), \qquad \text{(Eq. 2.8)}$$

where V is an appropriate velocity, y an appropriate flow depth, and $f(y/d_{50})$ represents a function of a relative depth. Equation 2.8 is evidently a generalization of Equation 2.7, and a large number of the riprap design equations examined in NCHRP-568, not only for streambank protection, but also for pier and abutment riprap applications, can be expressed as in Equation 2.8. The more common form involves $V/\sqrt{g(s-1)y}$, which can be interpreted as a type of Froude number (see NCHRP-568), but the above form involving $V^2/[g(s-1)d_{50}]$, interpreted as a type of bulk Shields parameter, is preferred as being more amenable to extension to the culvert-outlet case.

As an example, the equation recommended in NCHRP-568 for streambank protection is the U.S. Army Corps of Engineers or Maynord model, which in its basic form would read

$$\frac{V^2}{g(s-1)d_{50}} = 3.0\left(\frac{y}{d_{50}}\right)^{1/5}. \qquad \text{(Eq. 2.9)}$$

Because the original equation was formulated in terms of d_{30} rather than d_{50}, it has been assumed that $d_{50}=1.2d_{30}$ (see NCHRP-568) in writing Equation 2.9. If the equation recommended in Brown and Clyde (1989; also to be referred to as the HEC-11 equation) had been used, then the right hand side of the equation would be changed to $2.3(y/d_{50})^{1/3}$. In any case, as NCHRP-568 notes, in these design equations the effect of flow depth is rather weak (as reflected in the relatively small value of the exponent, 1/5, in Equation 2.9). This motivates a design equation in which the right hand side of Equation 2.8 is chosen as a constant, which leads back to Equation 2.7. A conservative choice based on Equation 2.9 would be $K=3$, which is consistent with the Isbash or Searcy version of Equation 2.7.

A list of states with agencies (predominantly but not necessarily departments of transportation) adopting one or other of the above-discussed approaches to riprap-apron design is given in Table 2.2. The list is not intended to be comprehensive; for some states, design guidance for simple riprap aprons was not specifically addressed, for others only a generic reference to HEC-14 (or other sources) is given or very rarely did not fit within the discussed approaches. Different agencies in the same state may adopt different approaches, and so the same state may appear more than once in Table 2.2.

2.4 A Synthesis (Framework) Equation and Comparison of Design Equations

As hinted at in the preceding section, Equation 2.8 may provide a starting point for a riprap design equation applicable to culvert outlets, as it was able to provide a basis for the current INDOT riprap design guidelines. Both the Bohan and the HEC-14 equations can be interpreted in terms of a modified form of Equation 2.8:

$$\left[\frac{V_{out}^2}{g(s-1)d_{50}}\right]_{crit} = f\left(\frac{y_{out}}{t_w}, \frac{d_{50}}{D}\right), \qquad \text{(Eq. 2.10)}$$

where y_{out} is the outlet flow depth, and the subscript, *crit*, has been added to emphasize that the right hand side is a critical or limiting value separating stable and unstable values. A prime consideration in the choice of variables to be included in Equation 2.10 was their ready availability. Whereas in the 1970's when the Bohan and the HEC-14 models were being developed it was quite inconvenient to estimate V_{out} and y_{out} for a circular culvert not flowing full, these can now be obtained in a straightforward manner from standard culvert-hydraulics software such as HY-8 or using a spreadsheet. Thus, like the Bohan but unlike the HEC-14 models, Equation 2.10 is based on V_{out} rather than the discharge, Q, as it is argued that V_{out} is more

TABLE 2.2
States with agencies adopting a specific riprap-apron design approach for circular culverts

Bohan (1970) and Variants	Fletcher and Grace (1972) and Variants	Outlet Velocity Only	USDCM
Kentucky, Illinois, Iowa, Maine, Maryland, Michigan, North Texas, Virginia, Minnesota	Colorado, Delaware, South Dakota, Minnesota	Connecticut, Minnesota, Tennessee	Colorado, Missouri

directly related to outlet-scour processes. Unlike the HEC-14 and the closely related USDCM models, both based on Q and so needing to adjust the diameter for supercritical flows, the use of V_{out} should make any resulting equation more insensitive to whether the culvert flow is subcritical or supercritical. Similarly, y_{out}/t_w is preferred to t_w/D as a measure of the influence of the tailwater, because it is more directly related to flow characteristics at or immediately downstream of culvert outlets.

A distinction should however be made between the actual outlet velocity, $(V_{out})_{act}$, and the standard estimate, V_{out}, e.g., as is computed in HY-8. The latter is evaluated assuming (for subcritical culvert flows) that the outlet depth, $y_{out}=y_c$, if $y_c/t_w>1$, or that $y_{out}=t_w$ if $y_c/t_w<1$. It is not entirely clear whether Bohan (1970) based his equation on the actual velocity, but in the following V_{out} will refer to the standard estimate as this is what is available in HY-8 results. In some of the experimental results from the present study, it was noted that the actual outlet depth differed from the HY-8 estimates of the outlet depth.

In HEC-14 Appendix D, a comparison of various stone-sizing equations is given in dimensional terms, i.e., for specific numerical values. Such a comparison while no doubt useful is limited in being based on the chosen values. An alternative dimensionless approach on Equation 2.10 is preferred here in that it is less specifically tied to chosen values, though needs some care in interpretation. This is illustrated in Figure 2.4, which shows the stability boundaries of the HEC-14 model for different values of d_{50}/D, i.e., Equation 2.3, and those for the current INDOT design guidelines. The HEC-14 curves in Figure 2.4 comply with the HEC-14 recommendation that Equation 2.3 be applied only in the range, $0.4<t_w/D<1$, and so the curves may have very limited extent. In Figure 2.4, the region above and possibly to the right of a given curve (boundary) represents unstable conditions for the riprap apron, while the region below and possibly to the left of a curve represents stable conditions. This is seen most easily as higher values of $V_{out}^2/[g(s-1)d_{50}]$ due to either higher V_{out} or lower d_{50} are associated with greater instability. Thus, for given d_{50} and D, e.g., such that $d_{50}/D=0.1$, conditions represented by the point A (i.e., for known values of V_{out}, y_{out}, and t_w, say from a HY-8 analysis) in Figure 2.4, would be considered as unstable according to the HEC14 model, as the point A lies *above* the $d_{50}/D=0.1$ curve. This would indicate that a larger stone would be required for stability, which would, for the same

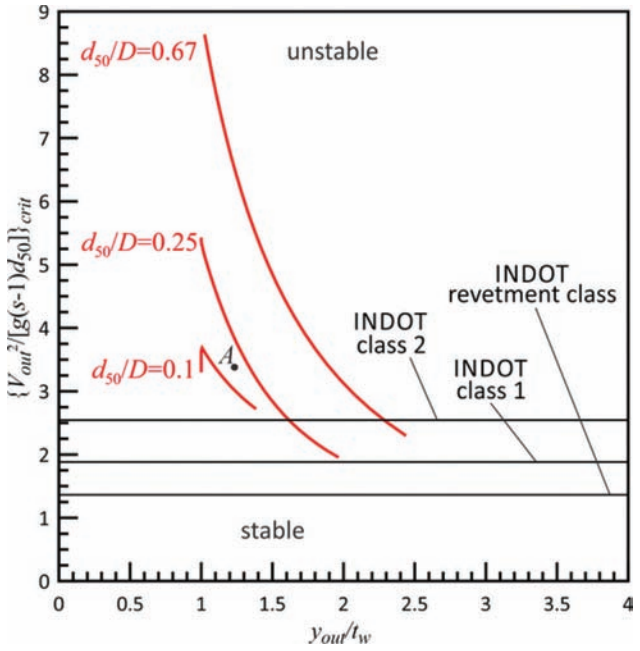

Figure 2.4 Comparison in proposed coordinates of the Fletcher-Grace-HEC14 model (red curves) for different d_{50}/D with the INDOT design guidance (black lines) for different standard riprap classes.

situation, not only reduce the value of $V_{out}^2/[g(s-1)d_{50}]$ i.e., move the point A downwards towards a stabler region, but also increases the value of d_{50}/D, and thus shifting the relevant stability boundary upwards, and hence enlarging the stable region. If the stone size is doubled such that $d_{50}/D=0.2$, then point A already lies *below* stability boundary curve for $d_{50}/D=0.2$, and so would represent a stable situation (point A would also move downward if d_{50} is increased).

The INDOT curves in Figure 2.4 were obtained by evaluating $V_{out}^2/[g(s-1)d_{50}]$ with the limiting value of V_{out} for the d_{50} of the respective standard riprap class. For example, for the revetment class, d_{50}, assumed to be 0.58 ft, and $V_{out}=6.5$ ft/s yielded $\{V_{out}^2/[g(s-1)d_{50}]\}_{crit}=1.36$. In Figure 2.4, the point A lies *above* the different stability curves for all three INDOT standard riprap classes, implying that it is unstable, but this should be qualified as for each riprap class, the point A corresponds to a different V_{out}. In practice, it would not be necessary to evaluate $V_{out}^2/[g(s-1)d_{50}]$ to determine riprap stability according to the current INDOT guidelines, so the comparison between the HEC-14 model and the INDOT policy is the main issue. For

small enough y_{out}/t_w, the HEC-14 curves lie above the INDOT curves, such that by comparison the latter are viewed as overly conservative, i.e., there would be points, such as point A, considered unstable by the INDOT guidelines that would be deemed stable by the HEC-14 equation.

As d_{50}/D increases, the HEC-14 curves shift upwards (and to the right), so that the stable region (below the curves) grows in size compared to the unstable region (above the curves). This is understandable because, for given D, increasing d_{50}/D means a larger stone, which would increase stability. On the other hand, the curve with the smallest d_{50}/D may be argued as being the most conservative as its stable region is the most restrictive, and so may be used even if, for given V_{out}, the resulting d_{50}/D is larger (but not smaller) than that associated with the smallest d_{50}/D.

The Bohan model is compared with the INDOT guidelines in Figure 2.5. As noted previously, unlike the HEC-14 model, the curves corresponding to the Bohan model do not vary with tailwater, *except* when at the transition point, $t_w/D=1/2$, and so they plot as horizontal lines that make a sudden jump at the transition point. Because y_{out}/t_w is preferred to t_w/D, the Bohan maximum-tailwater and minimum-tailwater conditions overlap, i.e., for some intermediate range of y_{out}/t_w, the chosen coordinates by themselves may lead to an ambiguity, and would still require examining t_w/D to resolve the ambiguity. The main qualitative features of the HEC-14 model are however found also in the Bohan model, namely that increasing d_{50}/D enlarges the stable region, shifting the stability curve upwards to the right, and high-tailwater conditions allow smaller stones to be considered stable that under low-tailwater conditions would be considered unstable. An aspect of the Bohan model compared to the HEC-14 model that will be relevant to the present study and so should be highlighted is the flatter variation of the curves. In Chapter 4, the proposed design curves will exhibit a flatter variation with y_{out}/t_w, and so might be viewed as intermediate between the Bohan and the HEC-14 models.

The Bohan minimum-tailwater curve for $d_{50}/D=0.1$, as the lowest curve in Figure 2.5, is more conservative than all three of the INDOT curves, whereas the other Bohan minimum-tailwater curves are generally less conservative. The somewhat conservative (at least for small d_{50}/D) Bohan minimum-tailwater curves may to some extent be explained by the conditions of his experiments. Bohan (1970) reported his minimum-tailwater data as being obtained under *zero*-tailwater conditions though this is likely an exaggeration. If, as in the HEC-14 model, $\{V_{out}^2/[g(s-1)d_{50}]\}_{crit}$ decreases continuously (though possibly weakly) with y_{out}/t_w, then a zero-tailwater condition would correspond to $y_{out}/t_w \to \infty$, such that lower and more conservative values of $\{V_{out}^2/[g(s-1)d_{50}]\}_{crit}$ would be expected. The much less conservative curve for large $d_{50}/D=0.67$ even compared to the HEC-14 model is not explained by this experimental aspect. The Bohan maximum-tailwater curves are all also less conservative than the INDOT curves, but it is surmised that this may also be due to the experimental method, as will be discussed in the next chapter.

For completeness, a comparison of the HEC-14 and the USDCM models is given in Figure 2.6. Except for smaller d_{50}/D, the USDCM model tends to be less

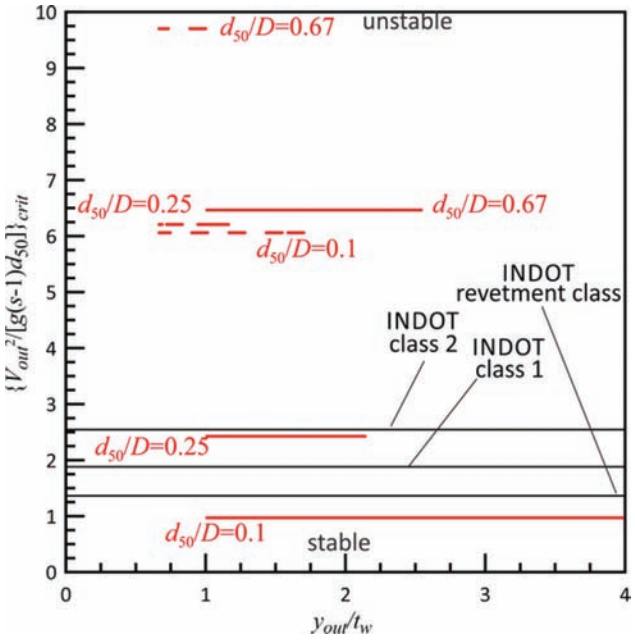

Figure 2.5 Comparison of the Bohan model (in red, full lines are for the minimum-tailwater condition, while dashed lines are for the maximum-tailwater condition) with the INDOT design guidance (black lines).

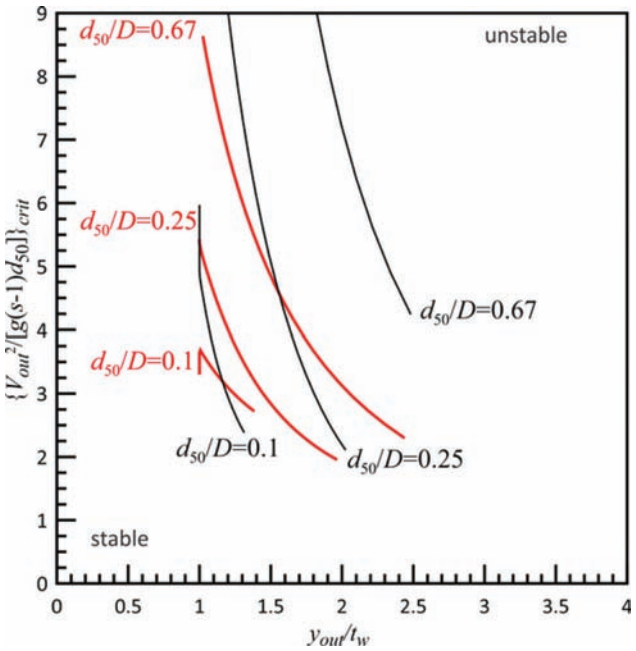

Figure 2.6 Comparison of the HEC-14 (red curves/labels) and the USDCM (black curves/labels) models.

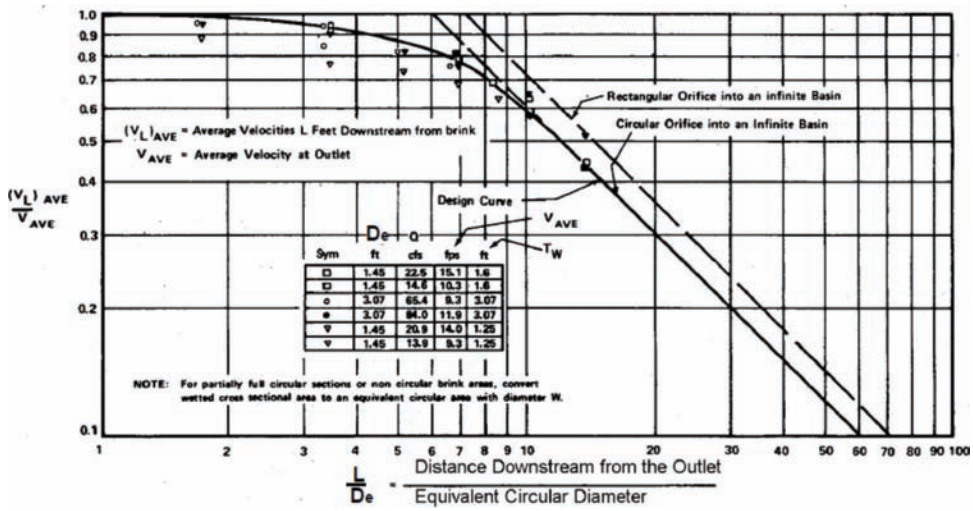

Figure 2.7 Reduction of (maximum) centerline velocity for flow from largely submerged culvert outlets (taken from HEC-14).

conservative than the HEC-14 model, as was previously found in the evaluation in HEC-14 Appendix D.

In the present study, curves similar to those seen in Figure 2.4 through Figure 2.6 will be developed based on experimental results. The equations will differ in detail but the general qualitative behavior will be similar. Whereas the HEC-14 model is defined by a single equation and the three curves in Figure 2.4 are selected for graphical purposes only, the proposed model will consist of a different equation for each curve. Each such equation/curve may be associated with a different level of conservatism to the extent that the lowest curve in the $V_{out}^2/[g(s-1)d_{50}] - y_{out}/t_w$ plane is the most conservative or restrictive in terms of d_{50}.

2.5 Velocity Behavior at Culvert Outlets

The present INDOT stone-sizing guidelines are based entirely on (outlet) velocity, and there is interest in the velocity behavior downstream of the culvert outlet. Figure 2.7, which is given in both HEC-14 as well the INDOT Design Manual (as Figure 203-2N), is intended to describe the decay of the jet velocity downstream of an outlet. As no reference is cited, the origin and the empirical details, such as whether the measurements were obtained with a rough or smooth surface, are not clear. Also, despite the figure label indicating that the velocity being characterized as the average velocity, it is interpreted (consistent with the figure caption in both HEC-14 and the INDOT manual) as the (maximum) centerline velocity. The results of Figure 2.7 imply that substantial velocity reduction is *not* to be expected within four diameters (the current INDOT guidelines for minimum apron length) of the outlet. Although an opposing view is sometimes seen in design manuals, the general consensus is that, as is stated in HEC-14, "These aprons do not dissipate significant energy except through increased roughness for a short distance." An interesting question, which will be examined in the present study, is whether, for quite large roughness (e.g., compared to the culvert diameter), a more significant dissipation could occur.

Figure 2.7 is also relevant to riprap-apron design, as HEC-14 proposed that it be applied for cases of high tailwater, $t_w/D>1$, i.e., above the recommended range of Equation 2.3. An estimate of the centerline velocity from Figure 2.7 can be combined with an Isbash-type equation (e.g., Equation 2.7) to evaluate an appropriate stone size. More directly, Figure 2.7 arises in the design of riprap basins (or energy dissipators) as discussed in HEC-14 (and the INDOT manual).

2.6 Summary

The features of the main alternative apron-riprap design approaches to stone sizing were reviewed and compared within a single framework with the current INDOT design guidelines. The latter were found to be quite conservative except in some cases of quite low tailwater depths, opening up the possibility of developing a design approach that would still lead to stable aprons using a smaller riprap class. Although not the main focus of the study, prescriptions for the apron configuration (length and width) were also reviewed, and it was noted that the current INDOT design specification of a minimum length of four diameters was situated at the low end of the spectrum compared to other models, including the HEC-14 recommendation. With implications for the apron length, the downstream variation of the maximum velocity was also discussed, together with the consensus view that a simple riprap apron was mainly intended to armor the bed and not to dissipate the energy of the outlet jet.

3. EXPERIMENTAL EQUIPMENT, DESIGN, AND PROCEDURES

In this chapter, the main experimental equipment used in the study is described, and the design of the experimental study is discussed. In addition, the general

procedure followed in obtaining the experimental results is detailed. The study of Bohan (1970) will frequently be referred to for comparison of experimental aspects with the current study. The basic data analysis, specifically a scoring system, to define operationally stable and unstable riprap aprons, and a regression approach to determine a stability curve separating stable and unstable parameter ranges, are sketched.

3.1 Experimental Equipment, Materials, and Instrumentation

3.1.1 The Laboratory Channel

The study was performed in a modified version of the channel used in the earlier JTRP study of culvert and bridge models (Lyn, Dey, Saksena, & Merwade, 2018). This report focuses on the main modifications made to the channel and flow system; other details may be found in Lyn et al. (2018). The main modification was the removal of the headwater section of the channel, such that the supply pipe, instead of discharging into a headwater section upstream of a culvert inlet, discharged directly into the pipe-culvert model (Figure 3.1). Whereas headwater measurements were essential in the earlier study, outlet scour was the focus of the present study, and only conditions at and downstream of the culvert outlet were considered relevant. In this respect, the present channel was similar to that of Bohan (1970).

In the Bohan study, experiments were performed with four pipe diameters (0.125 ft, 0.224 ft, 0.333 ft, and 1 ft), but the experiments with the 0.125-ft pipe were observed to exhibit extraneous scale effects, and the results from these experiments were not used. Based on the Bohan study, the two pipe diameters for this study were chosen to be 0.35 ft and 0.48 ft in order to avoid scale effects. At the pipe inlet, in most cases, one or two banks of straws were installed lengthwise to act as flow straighteners/conditioners in order to accelerate the transition from a bend flow to a nearly horizontal unidirectional culvert flow. In some cases, for the smaller-diameter pipe, pipe velocities were too large for the straw banks to be stable, and so in these cases, no straw bank was in place. The distance from the end of the bank of straws to the model culvert outlet could be $\approx$5 ft or $\approx$6 ft depending on whether one or two banks of straws were in place.

Common culvert outlet- (and inlet-) geometries, particularly for smaller culverts, include those in a headwall with or without wingwalls and those with a projecting pipe. All of the experiments in the present study were performed with the pipe outlet in a simple headwall (see Figure 3.1b). The outlet geometry of the Bohan study is not clearly specified, but the figures in the report suggest a pipe projecting out from a sloping face. The flow features immediately downstream of a pipe in a headwall and of a projecting pipe are not expected to be substantially different, especially from the point of view of the near-bed flow that is important for bed scour.

The width of the laboratory channel was 3.6 ft (Figure 3.2). Relative to the pipe diameters, the channel widths were $\approx 7.5D$ and $\approx 10D$; in comparison, in the Bohan study, the channel width was 16 ft, corresponding to $16D$ to over $70D$, depending on which pipe is considered. A consequence of the much larger width in the Bohan study is the capability of attaining quite low tailwater levels, as the lowest tailwater achievable is dictated by critical flow depth in the channel. The Bohan configuration is also likely more representative of discharges into an ill-defined channel.

As in Lyn et al. (2018), the pipe and channel are approximately horizontal, and so supercritical flow was never established in the pipe. For some discharges with the larger pipe diameter, at low tailwater depths, subcritical open-channel flow prevailed in the pipe for some distance, but in most cases, especially in those cases near the onset of apron instability, the pipe flowed full throughout its length, or the region of open-channel flow was very limited, often only a small fraction of a diameter. Bohan (1970) does not make any mention of subcritical or supercritical flow. As previously argued, if the most important variable in apron instability is the outlet velocity, then models formulated in terms of outlet velocity will be insensitive to whether the culvert

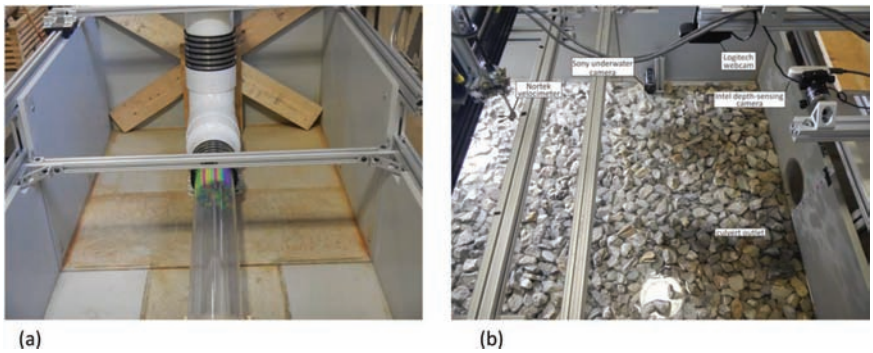

Figure 3.1 (a) Transition from the 8-in diameter supply pipe and bend to the model culvert pipe (in this case, 0.48-ft diameter and transparent, with one bank of colored straws at pipe inlet), (b) outlet of 0.48-ft model culvert pipe in a headwall with instrumentation and with undisturbed model bed/apron with 1.22-in stone.

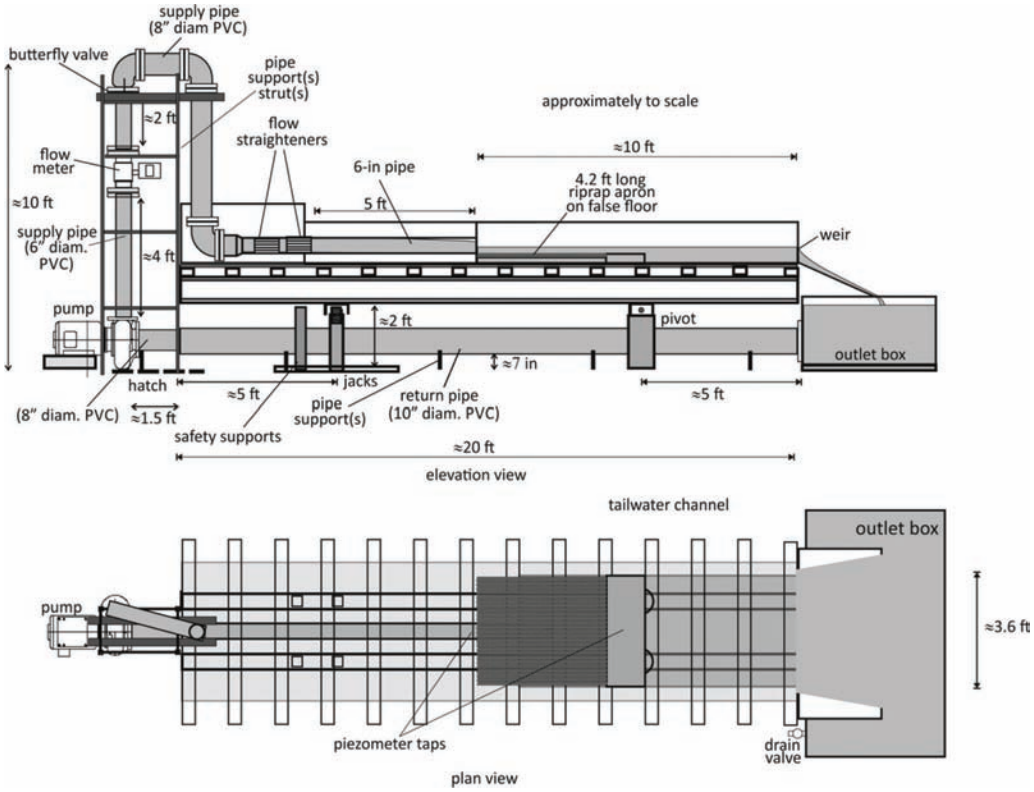

Figure 3.2 Sketch (elevation and plan views) of laboratory channel with the 5.75-in (0.48-ft) model pipe culvert (some dimensions and features differ with the 4.25-in pipe).

flow is subcritical or supercritical. Hence whether the model pipe flow is subcritical or supercritical will not be of primary importance as long as its velocity is known.

In order to minimize the amount of coarse aggregate material to be used, false floors were installed just downstream of the culvert outlet, the streamwise extents and elevations of which were varied depending on the pipe diameter and the stone size. For the 0.48-ft pipe, the model riprap extended a distance of 4.2 ft or 8.6D, while for the 0.35-ft pipe, the extent was 3.1 ft or 8.8D (Figure 3.2), both of which may be compared with the recommended INDOT minimum of 4D and the HEC-14 maximum of 8D. Because the Bohan study was aimed primarily at studying scour hole dimensions, its channel consisted of a 20-ft long 3.5-ft deep bed of fine sand (d_{50}≈0.22 mm) with surface on grade with the culvert invert, and terminating in an end sill, followed by a pool. As such, in the Bohan study, riprap was only placed in the area adjacent to the culvert outlet, based on results of prior scour-hole experiments. In the present channel, an end sill extending ≈1.1 ft farther downstream from the riprapped section, with top also on grade, was installed to simulate a downstream channel bed. A pool separated the end sill from the downstream weir, which was located, depending on the pipe diameter, either 10 ft (for the 0.48-ft diameter pipe) or 8 ft (for the 0.35-ft diameter pipe) from the culvert outlet. The height of the weir crest was varied to vary the tailwater elevation.

3.1.2 Materials: Model Riprap and Sand

Four coarse aggregate material of different size were used to model the riprap in the present study. The raw material was obtained from U.S. Aggregates (Delphi, IN), and then custom-sieved to obtain a relatively uniform model riprap. The different size classes were material (i) passing through the 0.75-in and being retained on the 0.5-in sieves, (ii) passing through the 1.5-in and being retained on the 1-in sieves, (iii) passing through the 2-in and being retained on the 1.5-in sieves, and (iv) passing through the 2.5-in and being retained on the 2-in sieves. An image of the differently sized material is shown in Figure 3.3. Because a more detailed size distribution for each fraction could not be performed, the d_{50} for each size class was estimated as the geometric mean of the two bounding sieve sizes, namely 0.61 in, 1.23 in, 1.73 in, and 2.24 in; because the bounding sieve sizes are close, the difference from an arithmetic mean is negligible. No attempt was made to mimic the gradation of the INDOT standard riprap, which is rather less uniform than the model riprap. In a review of riprap design, NCHRP-568 discussed the effects of gradation on riprap stability, stating that "Most studies suggest that a well-graded riprap layer is better suited to resist the winnowing of bed sediments compared to a layer that exhibits a uniform gradation." From this point of view, the use of a uniform model riprap might be considered as giving conservative results. NCHRP-568 did note one study that gave a differing conclusion.

Figure 3.3 Image of the typical coarse aggregate material used in study.

While the sieve size is the main characteristic of importance in riprap design, other characteristics such as the shape and the angularity may also influence riprap stability. In general, it was observed that as the size (d_{50}) increased, the material tended to become more angular and less spherical (see Figure 3.3). A higher degree of angularity is expected to increase the stability, as the USACE or Maynord equation as described in NCHRP-568 for streambank riprap sizing would suggest. The effect of shape and angularity may also be interpreted in terms of the friction angle or the angle of repose, in that a larger friction angle is associated with increased stability. The angle of repose tends to increase with increasing stone size, typically asymptoting to a constant value (Simons & Sentürk, 1992). As such, increases in stone size from the laboratory to the field scale are expected to lead to either increase in or at least negligible effect on stone stability.

In a limited series of experiments to examine scour downstream of the apron, a coarse sand was used to simulate a downstream erodible streambed. The sand was also relatively uniform, all passing through a no. 8 (2.36 mm) and being retained on a no. 16 (1.17 mm), for which d_{50} was estimated as 1.7 mm.

3.1.3 Instrumentation

For the riprap stability experiments, the main measurements were the discharge and the tailwater level.

An electromagnetic flow meter (Badger M2000) in the supply pipe (Figure 3.2) with a manufacturer specified accuracy of 0.25% of rate (for measured velocities greater than 1.6 ft/s, i.e., discharges greater than 0.3 cfs) was used. Water surface elevations were obtained with a digital point (depth) gage (Mahr Federal, MARCAL 30 EWR 4126702), with a manufacturer-specified resolution of 0.0005 in and accuracy of 0.002 in. In practice, at the larger discharges, the water surface could fluctuate substantially, and the measurement error or uncertainty was determined more by the decision as to the average water surface elevation.

A key aspect of the study was the visual detection of stone motion and hence riprap instability. Video records were made of the riprap apron exposed to the flow from the culvert outlet, and these could be subsequently inspected for stone motion. The advantage of video recording is that it allows repeated viewing, and thus enhanced and reproducible detection of stone motion. For low-tailwater conditions, e.g., $t_w/D<0.75$, it was found that an overhead camera was usually adequate to detect significant stone motion over the apron. Two cameras could be used for this purpose: a Logitech C920 webcam, or an Intel D435 Realsense camera, both with a resolution of 1920 by 1080 pixels at 30 fps (Figure 3.1b). The field of view of these cameras varied depending on the elevation at which each was mounted, with the Intel camera being mounted so that its resulting field of view was about 2.3 ft at the bed surface. At higher tailwater levels, the larger depths and larger surface disturbances at higher discharges combined to make visualization of the bed difficult for overhead-mounted cameras. As such, a Sony FDR X3000 camera, operated with a resolution of 1280 by 720 pixels at 30 fps, was installed underwater near the channel sidewall (recall that the channel sidewalls were opaque). The field of view on the channel centerline of the Sony camera was ≈2.3 ft (≈4.7D or ≈6.4D depending on whether the pipe diameter was 5.75 in or 4.25 in), so its fixed streamwise position was varied depending on the specific experimental conditions. The early experimental studies such as Bohan (1970) did not record and relied on direct visualization, presumably from above, and it is surmised that, as a consequence, may not have been as sensitive in the high-tailwater case in detecting stone motion. This may have contributed to their tendency in the Bohan model and to a lesser extent in the HEC-14 model to be less conservative in their stability curves for high-tailwater conditions.

Although the Intel D435 camera was sometimes used for video recording, its main purpose was to aid in setting up the model apron. Because the large stone size prohibited the use of a scraper, leveling the apron at a reproducible elevation was accomplished by hand, and it was necessary to check the elevation. Hence a means of quickly evaluating the elevation of a rough surface of some extent was required. The D435 is a stereoscopic depth-sensing camera, capable of 3-D imaging. According to the manufacturer, the depth accuracy of the Intel D435 is less than 1% of the range, so that when it is mounted ≈500 mm from a surface (as it was in the study), it should be able to measure with less than 5 mm error. It is believed that this specification is somewhat conservative in that differences in elevation of less than 2 mm could be detected. For the present study, measurement of absolute distances was of less concern than the ability of resolve differences in elevation.

Point velocity measurements were also made as part of the study. These were obtained by means of a Nortek Vectrino acoustic Doppler velocimeter (ADV) with a side-looking (2D-3D) probe (Figure 3.1b). The four-pronged probe, usually used with all prongs submerged, has an approximately cylindrical sampling volume that is 6 mm in diameter and 12 mm long, and located 5 cm

in front of the probe. According to manufacturer's specifications, the Vectrino is capable of measuring with an accuracy of 0.5% of the measured value plus or minus 1 mm/s. In practice, other factors such as turbulence and signal quality issues will likely increase the uncertainty in mean velocity measurements.

3.2 Experimental Design

The experiments were designed to investigate primarily the appropriate stone size for smaller (circular) culverts. More specifically, as the current INDOT design guidance chooses stone size solely on the basis of outlet velocity, the question was raised whether other factors such as the culvert size and the tailwater may influence riprap stability and hence could potentially justify the use of smaller stones. Hence, the experiments varied discharge, tailwater levels, stone size, and culvert diameter. Two pipe diameters (D=0.35 ft and 0.48 ft) and four stone sizes (d_{50}=0.61 in, 1.23 in, 1.73 in, and 2.24 in) were used. As the HEC-14 model is limited to $0.4<t_w/D<1$, it was of interest to examine the instability behavior beyond this range, so tailwater levels higher than the culvert crown and as low as could be achieved (typically this was limited by critical flow in the downstream channel). For a given stone size, culvert diameter, and tailwater level, a series of experiments were conducted in which the discharge was varied, starting from one well below the instability boundary, to one where a large part of the riprap apron was mobilized, hereafter to be termed the "catastrophic" failure condition. The parameter ranges covered in the present study as well as that of Bohan (1970) are compared in Table 3.1.

A secondary aim of the study is related to the streamwise extent or length of the riprap apron. The current INDOT design guidance of a minimum of 4D independent of flow conditions is situated at the low end of the HEC-14 recommendation (see Table 2.1), which varies with stone size, and is notably smaller than that given by the Bohan (or HEC-14) model. What are the implications for the apron length, within the specific context of smaller culverts and larger stone sizes? Although some limited experiments were conducted studying the scour of a downstream section of finer model streambed material, the main focus with regards to apron length was placed on the streamwise evolution of the mean velocity field. Since it was thought that the main effect on the velocity would be due to the roughness of the apron, point velocity measurements were taken only for the largest stone size, i.e., largest roughness, with the smaller pipe diameter. Velocity profiles in the cross-stream direction at different streamwise sections were taken under a high and a low tailwater condition at the same nominal discharge, and for the low-tailwater condition, at two different discharges.

TABLE 3.1
Range of parameter values in the experimental study

	t_w/D	y_{out}/t_w	d_{50}/D	$Q/\sqrt{gD^5}$	$V_{out}^2/[g(s-1)d_{50}]$
Present Study	0.13–1.7	0.6–4	0.1–0.5	0.07–2.6	0.1–15
Bohan (1970)	0, 1	n/a	0.06–1	0.04–3.9	2.7–19.8

Notes:

(i) The values for the Bohan study are those only for the stone-sizing experiments (from his Table 2); thus, Bohan (1970) reports the tailwater as 0 D and 1 D, though zero tailwater is unlikely to be realistic.

(ii) V_{out} for the Bohan (1970) is computed from the reported outlet Froude number, $V_{out}/\sqrt{gD}$, and may not be the same as that used for the present study.

3.3 Experimental Procedures and Details

3.3.1 Riprap-Apron Stability Experiments

In preparation for a series with a given stone size (d_{50}), the downstream false floor was placed at an appropriate elevation. In general, the model riprap had at least two layers of stone, though the total apron thickness was typically less than $2d_{50}$. The main interest lay in the motion of the topmost stone layer (so not for bed protection), and so the apron thickness is not considered important in itself, but only that a lower layer exists in order to provide the appropriate support and resistance to stone motion. In most experiments, the apron covered the width of the channel, except for a region adjacent to one sidewall where the underwater camera was mounted (see Figure 3.1b). In experiments with d_{50}=1.73 in (and the smaller pipe diameter), the apron covered a more restricted region, similar in general shape to those shown in Figure 2.3 with a streamwise flare of ≈1:3. With the apron geometry and the nominal tailwater level decided, an experimental run consisted of varying the discharge with a fixed downstream weir crest height. The typical procedure for such a run would include:

- *Apron preparation:* The apron was hand leveled. For the smaller material, this involved only tamping by hand, but for the larger material, individual stones might need to be rearranged in addition to an initial hand-tamping. The Intel D435 camera provided estimates of the mean and standard deviation of the elevation, as well as the angle relative to the camera (zero degrees corresponding to a perpendicular surface) of a rectangular imaged region of the apron surface. The mean apron elevation was located at or slightly below that of the culvert outlet invert and the standard deviation was typically ≈0.2d_{50} and so the tops of isolated stones did protrude above the culvert invert.
- *Starting the flow:* For smaller material that might be susceptible to being mobilized during flow startup, the channel was filled to the weir crest level prior to the start of the flow through the culvert model. For the same reason, in some cases, the downstream weir crest was initially set to a high level, and only after the flow was started was the weir crest level reduced to the desired level. For larger material that was not likely to move under flow startup, the channel was filled by a low flow

through the culvert, and once there was flow through the channel, the discharge was increased slowly until the desired starting discharge was reached. The starting discharge was chosen to be well below that which would cause stone motion.

- *Video recording:* When a flow was established, in most cases, both an overhead and the underwater camera were started and recorded for at least ten minutes. This allowed stone-motion events to be detected from two different perspectives. In many cases, when both cameras were used, the start of video recording was staggered, so that the overhead camera recording was started during the transition from one discharge to another, while the underwater camera recording was started only after a desired discharge was established. Bohan (1970) did not specify the duration of his stone-sizing stability experiments, but did report 20-min duration for his apron-configuration experiments, in which scour outside of the apron was monitored.
- *Water surface and discharge measurements:* Once a desired discharge has been reached, the discharge was recorded along with the tailwater level. The tailwater was measured at a point ≈1.7 ft downstream of the culvert outlet at a point outside of the jet region, ≈0.5 ft from the sidewall. During the duration of the video recording, observations would be made of the flow in the pipe, e.g., the length of free-surface-flow region and the approximate level of the free surface at the culvert outlet, and whether any stone had moved onto the end sill or even farther downstream.
- *Incrementing the discharge:* After the video recording at a desired discharge, the discharge was incremented, and the above procedure repeated for a new higher discharge. This was continued until a discharge was reached, which resulted in substantial stone motion over an extensive region, usually with the apron being scoured out to the false floor bottom, i.e., what has been termed "catastrophic" failure.

3.3.2 Experiments to Obtain the Mean-Velocity Field

Experiments in which point velocity measurements were made started in the same manner as the riprap-stability experiments with the preparation of the apron and starting the flow. Neither discharge nor tailwater was however varied during any single run, but could be varied between runs. Mean velocities at a point about mid-depth (at $\approx 0.4\ t_w$) were instead measured with the Nortek Vectrino velocimeter. The discharge was chosen to be below that which would cause stone motion, which might damage the velocimeter (the probe of which had to be submerged, and was positioned at a height such that a moving stone could collide with the probe). At each point, three components of the instantaneous velocity vector were sampled at a rate of 20 Hz for a duration of 75 seconds. Transverse profiles at various streamwise sections (at distances of $x/D=0.41$, 2.29, 5.11, and 8.9, where x is the streamwise distance from the culvert outlet, and $D=0.35$ ft) were taken at a single elevation at approximately half depth. The entire duration of an experiment was approximately 2–3 hrs.

3.4 Data Analysis

Data analysis focused on identifying a riprap-stability boundary, which requires an operational definition of riprap instability from the recorded video clips. While it could be argued that the motion of a single particle is a precursor to apron instability, an isolated particle becoming mobile may be an outlier, perhaps due to its being at the small end of the size distribution, or being especially exposed to the turbulent flow and hence being more susceptible to being mobilized. Further, the displacement of an isolated particle does not necessarily threaten the integrity of the apron as a whole. Thus, as Bohan (1970) stated, "In several cases only one or two stones were displaced and no other stone movement occurred. This was not considered failure." On the other hand, defining the critical condition as that where a substantial fraction of the apron is mobilized would, in most estimation, go beyond what would be tolerated as a safe design.

In the Bohan study, ". . . the condition at which several stones were displaced from the upper layer of the two-stone-diameter-thick blanket would be termed failure," though how many stones were "several" was not specified precisely. In the present study, the apron condition is defined in terms of the number of (independent) mobilization events rather than the number of mobilized particles. It was observed that the motion of multiple particles in approximately the same location may be initiated during a single event, presumably because the motion of one particle caused other particles in the same region to move at or about the same time. Hence, a criterion based on number of particles moved may be misleading. The number of independent mobilization events observed during the record will vary to some extent with the duration of the observation period, and the choices made in this study are specific to the approximately 10-min duration of the video clips.

To evaluate apron-stability, a two-step scoring system was applied to each video record of a single experimental condition (discharge, tailwater level, pipe diameter, and stone size). In the first step, each video record was examined independently of other conditions; specifically, those immediately preceding records with lower discharges were not taken into consideration (recall that a series of experimental runs is conducted with only the discharge being incremented). A score of -1 was assigned to a case where no mobilization event was observed during the entire record, a score of 0 assigned if only a single mobilization event was observed, a score of 1 if more than one event was observed, and a score of 2 if a catastrophic failure condition (when the apron is scoured out to the false floor) occurs.

The results of this first step are subject to an inconsistency because the first step considers each case or record in isolation, and neglects prior cases in the series of experimental runs of increasing discharge. It is possible that an event is observed during one run, but in the

subsequent run at an increased discharge, no event is observed. The scoring after the first step would then assign 0 to the prior run, and then -1 to the subsequent higher-discharge run, but, under the same conditions, the higher-discharge run would also have caused an event that the prior lower-discharge run had caused, and therefore should at least be assigned an equal score. The principle was therefore followed that, in a series of runs with increasing discharge, the final assigned score to a case cannot decrease, so in the above case, the score for the higher-discharge run was adjusted to 0 in the second step to be consistent with the score of the prior lower-discharge run. Further refinements to the scoring system were considered but for the present purposes the above was deemed sufficient.

The scoring system is illustrated in Figure 3.4, where the results are presented for four series of experiments with the 4.25-in pipe and the 2.24-in stone, so that $d_{50}/D=0.53$. The data for each series are circled (full lines), with the lowest point at the smallest Q (and hence smallest $V_{out}^2/[g(s-1)d_{50}]$) chosen such that there is no mobilization event (for a score of -1), and each subsequent higher point (in a circled region) with a higher $V_{out}^2/[g(s-1)d_{50}]$ from the incremented discharge, and so on, until the final point (in red), at the highest $V_{out}^2/[g(s-1)d_{50}]$, when "catastrophic" failure occurs. As Q is incremented, the sequence of points moves approximately vertically because the downstream weir is set at a fixed elevation so that y_{out}/t_w is approximately constant, and point scores (within circles) typically from -1 to 0 to 1 and ultimately to 2. As seen in Figure 3.4, however, point scores may in some cases jump from 0 to 2, or from -1 to 1.

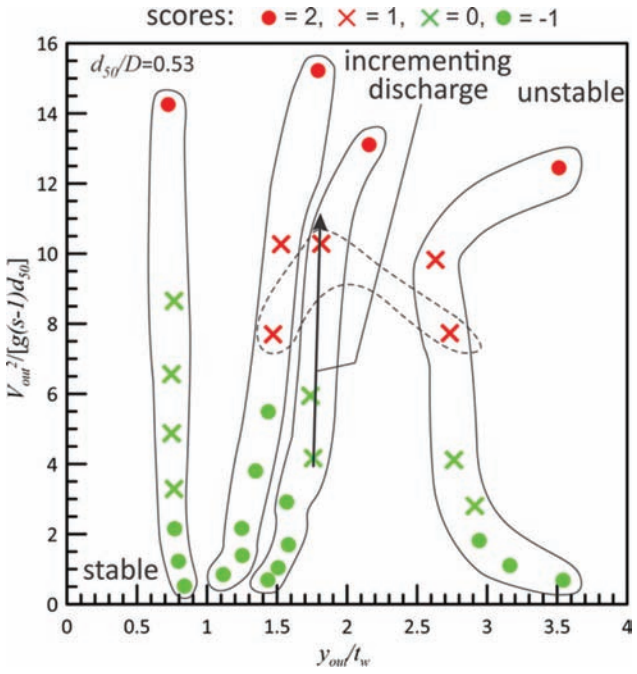

Figure 3.4 Experimental results illustrating scoring system (each of four series with incrementing discharge is circled in full lines, the "least" unstable points in each series are circled with dashed line).

The quantitative criterion for instability still remains to be defined. For simplicity, it was decided to apply logistic regression to determine the quantitative stability boundary. Although not commonly found in the hydraulics literature, logistic regression is discussed in Lyn and Tripathi (2017) where it is applied to a sediment-transport problem. Logistic regression assumes a binary behavior, i.e., the apron is either stable or unstable, with a sharp demarcation between the two possible states. This is implicitly the treatment in previous studies of riprap instability. For the at least 10-min video records, it was decided that points with a score (after the second step) of 1 or higher, i.e., at least two independent mobilization events occurring within the observation period, would be classified as unstable (all red symbols in Figure 3.4), and scores of 0 or lower classified as stable (all green symbols in Figure 3.4). This choice is considered reasonably conservative, as the value of $V_{out}^2/[g(s-1)d_{50}]$ at the resulting transition from stable to unstable was on average less than 60% of the corresponding value under catastrophic-failure condition (see Figure 3.4). In Figure 3.4, the "least" unstable point in each series, i.e., that after the stability boundary has "just" been crossed, is circled with a dashed line.

To determine the stability boundary from data such as those in Figure 3.4, the more usual approach would involve identifying the stable-unstable transition, such as the least unstable points circled with the dashed line (or alternately, the highest or most stable points could have been used) in each series. A conventional (linear or nonlinear) regression could then be applied to fit a curve to *only* these stable-unstable transition points, not to all of the stable and unstable points. Strictly speaking, the points identified (circled in dashed line) are *not* marginally stable—those points circled in dashed line in Figure 3.4 represent conditions where the marginally stable condition has already been exceeded. Thus, the conventional approach based on identifying transition points in this manner already makes an approximation. The chosen logistic regression does not rely on identifying stable-unstable transition points in the above manner but instead requires only the identification of stable and unstable points, yet still results in a type of "best-fit" curve that separates stable and unstable points. Thus, logistic regression uses all of the points, both stable and unstable, in determining the stability boundary. The exact details of the models assumed for the logistic regression will be discussed in the next chapter.

3.5 Summary

The experimental apparatus and instrumentation used in the study were specified, and the design of the experiments conducted was discussed in relation to the aims of the study and also to the earlier study of Bohan (1970). An outline of the typical experimental

procedure for both the stone-sizing and the velocity-field experiments was given. The data analysis and specifically how apron stability can be operationally defined were described and the statistical technique for obtaining the curve separating stable and unstable regions was introduced.

4. RESULTS

In this chapter, experimental results regarding apron stability are presented along the lines suggested by the synthesis (or framework) equation of Chapter 2.4. Stone-sizing equations based on a logistic-regression analysis of the experimental data, as well as a procedure for applying the equations are proposed. The proposed equations and procedure are then applied to a sample of actual culverts, and the results in terms of the minimum standard INDOT riprap class are compared to the recommendations according to the current INDOT design policy, and to the other major design approaches. Finally point velocity measurements are presented and implications for the apron length are discussed.

4.1 Qualitative Observations

Before more quantitative results are presented, some qualitative observations may be given. The Bohan model emphasized the distinction between low-tailwater (or minimum-tailwater) and high-tailwater (or maximum-tailwater) conditions. For smaller stone sizes, the present study also found striking differences, particularly in the scour behavior, between the two conditions. Selected photographic images of the scour pattern in the apron after catastrophic failure has occurred are shown in Figure 4.1 for higher-tailwater and lower-tailwater conditions with different stone sizes. Note the change in camera angle between Figure 4.1a and b (camera looking upstream to the outlet) and the others (camera from above looking to the side). The scour pattern under higher-tailwater conditions tends to be narrower and more elongated, with the scour hole starting at a farther distance from the outlet and usually extending all the way to the end sill (where the expanded-metal sheet lies on the surface–for both pipe diameters, the end sill starts at $\approx 9D$ from the culvert outlet, so the streamwise length of the apron is $\approx 9D$). These

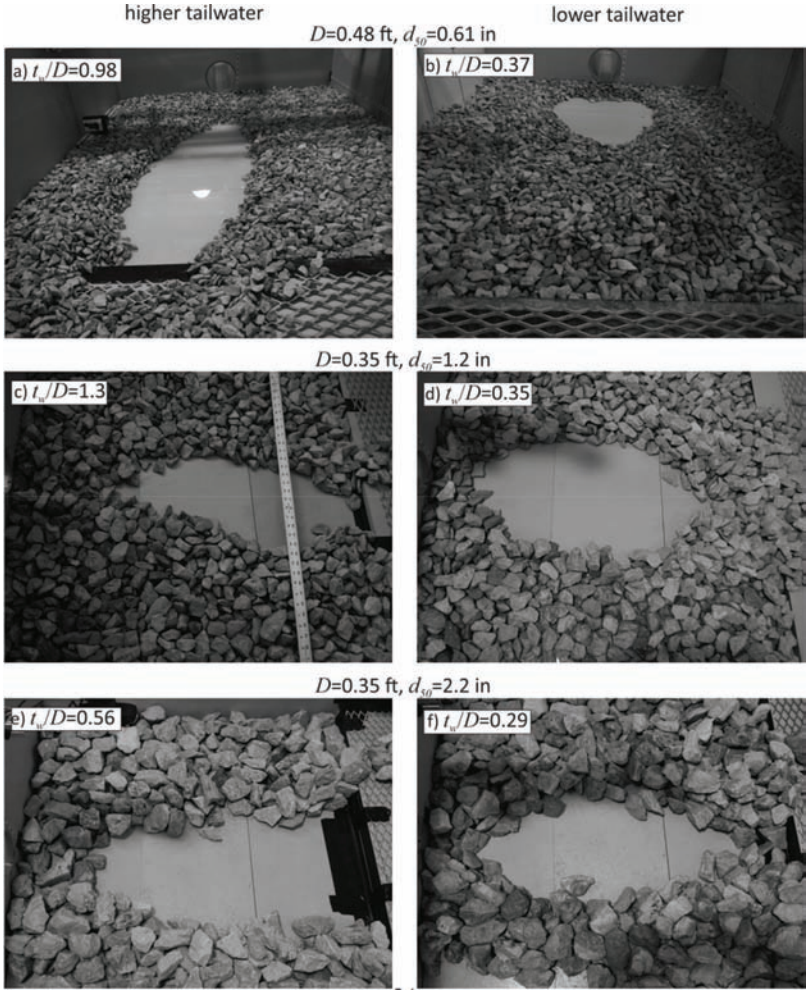

Figure 4.1 Scour patterns after catastrophic failure of the apron has occurred for higher-tailwater (on the left) and lower-tailwater (on the right) conditions for various different stone sizes (and pipe diameters).

observations generally agree with those of the Bohan study, which noted that "The jet from the culvert dispersed rapidly with minimum tailwater and required a short, wide blanket; however, with maximum tailwater, the jet traveled a considerable distance downstream and required a long, narrow blanket to prevent erosion."

The results in Figure 4.1 provides, however, a more nuanced view than that of the Bohan study. As the (relative) stone size (say d_{50}/D) increases, the differences between the higher-tailwater and the lower-tailwater cases diminish. The contrast in the streamwise extent of the scour holes in Figure 4.1a and b is striking for the smallest stone, but is much less so for the larger stones. For the largest stone (Figure 4.1e) the tailwater level is relatively low (though still technically a maximum-tailwater condition in the Bohan classification) but the scour hole geometry is decidedly similar to the cases with significantly higher tailwater levels. This is attributed mainly to the larger $V_{out}^2/[g(s-1)d_{50}]$ required for catastrophic failure for larger stones under low-tailwater conditions, the effect of which extends farther downstream such that the scour hole also extends farther downstream. The above applies to conditions resulting in catastrophic failure, but are expected to hold at least qualitatively for much less severe conditions.

Another aspect that was also noted in the Bohan study was the tendency of the jet flow from the outlet to move away from the centerline under high-tailwater conditions. According to Bohan (1970), "With maximum tailwater, the jet also changed position from side to side." Although an oscillation of the jet from side to side was not observed in the present study, a tendency for the jet to move away from the channel centerline was noted for high-tailwater cases. The stronger asymmetry with respect to the channel centerline is evident in Figure 4.1 for the higher-tailwater case. Related to this is a downstream surface circulation that was strongest under higher-tailwater conditions but largely disappeared under the lowest-tailwater conditions. Such a circulation, if mainly a surface phenomenon, should not affect stone stability.

4.2 Stone Stability Results

The results for the smallest stone (d_{50}=0.61 in) with two different pipe diameters (D=0.35 ft and 0.48 ft) are shown in Figure 4.2. The fact that the results with different pipe diameters agree well gives support to the chosen scaling. The dependence of stability on tailwater conditions when $y_{out}/t_w>1$ is especially evident with a sharp rise in the value of $V_{out}^2/[g(s-1)d_{50}]$ needed to cause catastrophic failure (score = 2). This is no doubt related to the "step"-like distinction in the Bohan model between a minimum- and maximum-tailwater condition. If however the stability boundary is defined at the lowest value of $V_{out}^2/[g(s-1)d_{50}]$ leading to a score of 1 (more than one mobilization events and recalling Figure 3.4), as is done here, then the variation in the same range, $y_{out}/t_w>1$, is notably milder. For $y_{out}/t_w<1$

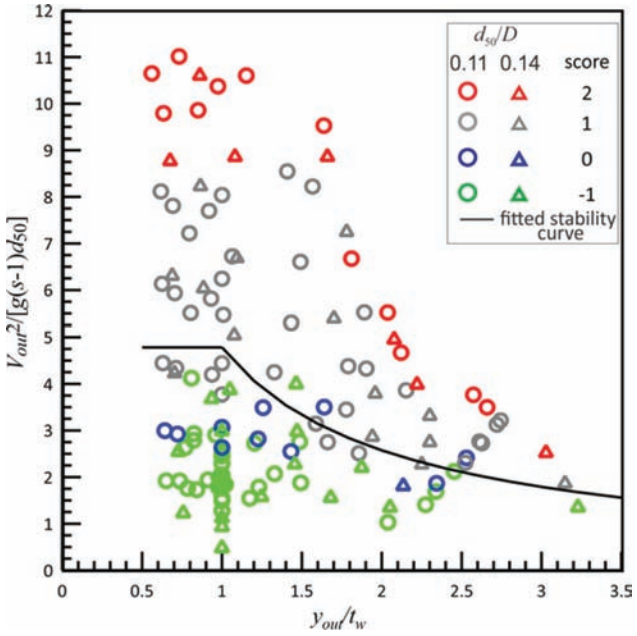

Figure 4.2 Stability scores for experiments with the smallest stone (d_{50}=0.61 in) with two different pipe diameters (D= 0.35 ft and 0.48 ft) together with the fitted stability boundary curve.

the variation becomes much flatter, again especially evident for the catastrophic-failure cases. Points for which $y_{out}/t_w<1$ arise mainly but not solely when the pipe outlet is submerged, and as the tailwater increases beyond a certain level after submergence, the effect of the tailwater level on apron stability should become negligible. Also drawn in Figure 4.2 is the "best"-fit regression curve separating stable (those points with scores of 0 or less) and unstable (those points with scores of 1 or more) regions that will form the basis of a proposed stone-sizing procedure. Details of how this and other similar curves are constructed are discussed in the next section. For now, the curve is seen to perform well in separating stable (below the curve) and unstable (above the curve) points. A number of unstable points (gray circles) are nevertheless seen located *below* the curve and a few stable points (blue circles) are situated above the curve, which is expected from a "best"-fit regression curve to scattered data. A means of dealing with these "incorrectly" identified unstable points will also be dealt with in the next section.

The corresponding results in Figures 4.3 and 4.4 for the other stone sizes exhibit generally similar behavior as was seen for the smallest stone (note the change in the vertical scale). The scatter particularly for the catastrophic-failure (score = 2) cases is greater, especially for the largest stone (Figure 4.4), though the latter may be due to the fewer data points and possibly a greater sensitivity to stone size. Despite the scatter, a tendency may be seen for larger $V_{out}^2/[g(s-1)d_{50}]$ for the same score at the same y_{out}/t_w, agreeing qualitatively with both the Bohan and the HEC-14 models (recall Figures 2.4 and 2.5). The stability curve for the medium stone is

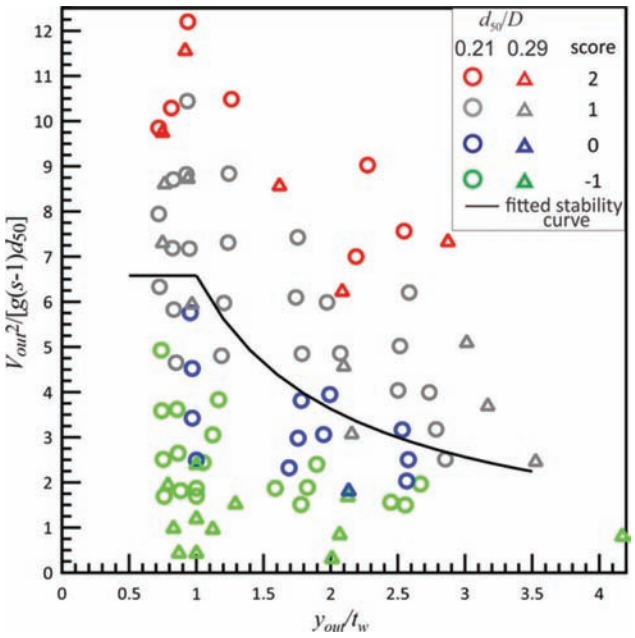

Figure 4.3 Stability scores for experiments with the medium stone (d_{50}=1.22 in) with two different pipe diameters (D= 0.35 ft and 0.48 ft) together with the fitted stability boundary curve.

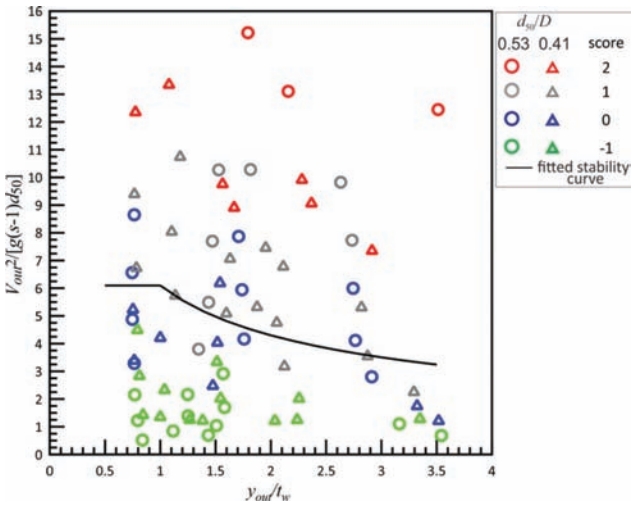

Figure 4.4 Stability scores for experiments with the largest stones (d_{50}=1.73 in and 2.24 in) with a single pipe diameter (D=0.35 ft) together with the fitted stability boundary curve.

similar in shape but shifted upwards to that previously seen for the smallest stone, but that for the largest stones seems to vary more gradually for $y_{out}/t_w>1$.

4.3 Regression Analysis

Previous work such as Bohan (1970) developed equations for apron stone sizing from identifying a limiting unstable stone size for given flow conditions, and then applying regression or equivalent. Such an approach uses uncertain information only from relatively limited set of data points. In contrast, in the present study, an alternative regression approach is preferred in which a much larger body of data points contributes to the proposed equations. This approach applies (linear) logistic regression in which *all* of the data points (though perhaps for a restricted range) are classified as being either stable or unstable, and a "best-fit" curve that best separates the two classes (stable and unstable) of data points is determined. It is emphasized that the logistic regression aims to find the best delineation of the stable-unstable transition, and does *not* find the best-fit curve to *all* of the points, e.g., as in Figures 4.2, 4.3, or 4.4.

As in other simple regression approaches, a candidate model equation and a range of application need to be specified. From a preliminary examination of the data, it was observed that the critical values of $V_{out}^2/[g(s-1)d_{50}]$, separating stable and unstable points, to be denoted as $\{V_{out}^2/[g(s-1)d_{50}]\}_{crit}$, varied more strongly with $y_{out}/t_w>1$, and varied weakly if at all with $y_{out}/t_w<1$. Hence, a model equation with the critical value of $V_{out}^2/[g(s-1)d_{50}]$ being constant for $y_{out}/t_w<1$, varying only for $y_{out}/t_w>1$ was considered. In the variable range, $y_{out}/t_w>1$, a power-law variation, somewhat similar to the HEC-14 model, was chosen, as this permits a linear model through a log-transformation. The model to be considered is thus

$$\left[\frac{V_{out}^2}{g(s-1)d_{50}}\right]_{crit} = a\left(\frac{y_{out}}{t_w}\right)^b, \qquad \text{(Eq. 4.1)}$$

where the coefficient, a, and exponent, b, are determined in the regression. After log-transformation, this becomes

$$\log\left[\frac{V_{out}^2}{g(s-1)d_{50}}\right]_{crit} = \log a + b\log\left(\frac{y_{out}}{t_w}\right), \qquad \text{(Eq. 4.2)}$$

which is linear in the fitting parameters, a and b, thus simplifying the regression. The constant value of $\left[V_{out}^2/\{g(s-1)d_{50}\}\right]_{crit}$ to be applied in the range $y_{out}/t_w \le 1$ is then chosen equal to a for continuity. The generic base model for apron stone stability may then be specified as

$$\begin{aligned}\left[\frac{V_{out}^2}{g(s-1)d_{50}}\right]_{crit} &= a, \text{ if } y_{out}/t_w \le 1,\\ &= a\left(\frac{y_{out}}{t_w}\right)^b, \text{ if } y_{out}/t_w > 1.\end{aligned} \qquad \text{(Eq. 4.3)}$$

The choice of a constant model for "high-tailwater" conditions ($y_{out}/t_w \le 1$) may be viewed as being similar to the Bohan model, except that a high tailwater is defined in terms of y_{out}/t_w rather than a maximum-tailwater condition defined in terms of t_w/D.

Although a model with the parameters, a and b, varying continuously with d_{50}/D was considered, a simpler model was preferred in which different regression curves with different parameters, a and b, were found for different ranges of d_{50}/D. Three curves were deemed sufficient to span the practical range of d_{50}/D,

TABLE 4.1
Logistic regression results for the fitting parameters for the different experimental ranges of d_{50}/D

Fitting Parameters	Data Range of d_{50}/D for Regression		
	$0.1<d_{50}/D<0.2$	$0.2<d_{50}/D<0.4$	$d_{50}/D>0.4$
a	4.783	6.578	6.099
b	-0.894	-0.858	-0.504

and so the experimental data were divided into three ranges, $0.1<d_{50}/D<0.2$; $0.2<d_{50}/D<0.4$; and $d_{50}/D>0.4$. The results of the regression for the different ranges d_{50}/D are summarized in Table 4.1, and the model curves have been included in the respective figures (Figures 4.2 through 4.4). The three curves are also compared in Figure 4.5, which shows that, as d_{50}/D increases, the stability curve tends to shift upwards, similar to the behavior seen in Chapter 2.2 in the HEC-14 and Bohan models. A curious feature inconsistent with this general tendency is the behavior of the curve for the range, $0.2<d_{50}/D<0.4$ and $y_{out}/t_w\leq 1$, which is *less* conservative than that for the larger range, $d_{50}/D>0.4$. This will be further discussed and dealt with in the next section.

4.4 Proposed Stone-Sizing Equations

The proposed stone-sizing equations are based on the regression results presented above. The inconsistent behavior for the curve for the range, $0.2<d_{50}/D<0.4$ and $y_{out}/t_w\leq 1$, is dealt with by restricting its application to a range such that it is always more conservative than the curve for the larger range, $d_{50}/D>0.4$. The two curves are found to intersect at $y_{out}/t_w=1.238$, and so the regressed curve for $0.2<d_{50}/D<0.4$ is only applied to $y_{out}/t_w\geq 1.238$ rather than to $y_{out}/t_w\geq 1$, and the constant part is conservatively extended up to $y_{out}/t_w=1.238$. The revised result is shown in Figure 4.6 as the red dashed curve.

4.4.1 Design Equations for Apron Stone Sizing

As noted, the "best"-fit curves directly from the regression result in several unstable points being located "below" them. Some of these points may be due to random experimental scatter, but their presence does make use of these raw equations problematic for design purposes. This is addressed by incorporating a safety factor, $C_{SF}\geq 1$ in the design equations. The following equations are therefore proposed for riprap-apron stone sizing, each based on a different data range:

$$(d_{50})_I=\left[\frac{V_{out}^2}{g(s-1)}\right]\begin{cases}\dfrac{C_{SF,I}}{4.78}, & \dfrac{y_{out}}{t_w}\leq 1,\\ \dfrac{C_{SF,I}}{4.78(y_{out}/t_w)^{-0.89}}, & \dfrac{y_{out}}{t_w}\geq 1\end{cases}\quad \text{for } \frac{d_{50}}{D}>0.1 \tag{Eq. 4.4}$$

$$(d_{50})_{II}=\left[\frac{V_{out}^2}{g(s-1)}\right]\begin{cases}\dfrac{C_{SF,II}}{5.47}, & \dfrac{y_{out}}{t_w}\leq 1.24,\\ \dfrac{C_{SF,II}}{6.58(y_{out}/t_w)^{-0.86}}, & \dfrac{y_{out}}{t_w}\geq 1.24\end{cases}\quad \text{for } \frac{d_{50}}{D}>0.2 \tag{Eq. 4.5}$$

$$(d_{50})_{III}=\left[\frac{V_{out}^2}{g(s-1)}\right]\begin{cases}\dfrac{C_{SF,III}}{6.1}, & \dfrac{y_{out}}{t_w}\leq 1,\\ \dfrac{C_{SF,III}}{6.1(y_{out}/t_w)^{-0.5}}, & \dfrac{y_{out}}{t_w}\geq 1.\end{cases}\quad \text{for } \frac{d_{50}}{D}>0.4 \tag{Eq. 4.6}$$

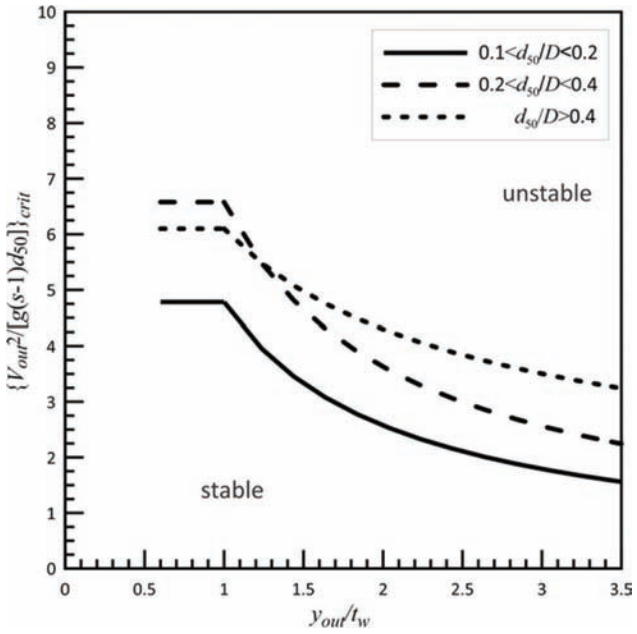

Figure 4.5 Comparison of regression results for the stone-stability curves for data from different ranges of d_{50}/D.

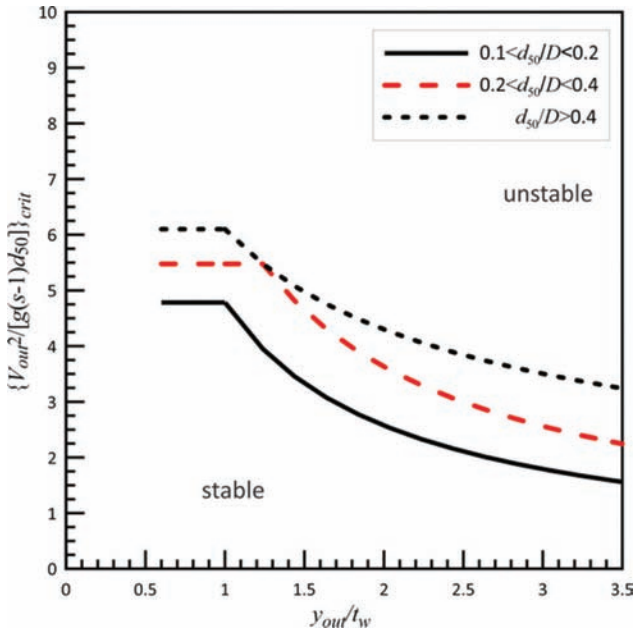

Figure 4.6 Stone-stability curves for different ranges of d_{50}/D (same as in Figure 4.5 except for the revised curve highlighted in red for the range $0.2<d_{50}/D<0.4$).

where different safety factors may be chosen for each equation and where the range of application of each equation based on the experimental data included in the determination has been specified. These can also be expressed more compactly and also more directly implementable in a spreadsheet as

$$(d_{50})_I = \frac{C_{SF,I}}{4.78}\left[\frac{V_{out}^2}{g(s-1)}\right]\max\left[1,\left(\frac{y_{out}}{t_w}\right)^{0.89}\right],\ (d_{50})_I > 0.1D,$$

$$(d_{50})_{II} = \frac{C_{SF,II}}{6.58}\left[\frac{V_{out}^2}{g(s-1)}\right]\max\left[1.2,\left(\frac{y_{out}}{t_w}\right)^{0.86}\right],\ (d_{50})_{II} > 0.2D,$$

$$(d_{50})_{III} = \frac{C_{SF,III}}{6.10}\left[\frac{V_{out}^2}{g(s-1)}\right]\max\left[1,\left(\frac{y_{out}}{t_w}\right)^{0.5}\right],\ (d_{50})_{III} > 0.4D.$$

(Eq. 4.7)

Although each equation is based on a different data range, they together form an ordered system in that each is more conservative that the next, and so can be applied to the range of the next. Thus, for example, in Figure 4.6, over the practical range of y_{out}/t_w, the curve (and equation) corresponding to $(d_{50})_I$ and based on data in the range $0.1<d_{50}/D<0.2$ is the lowest and hence most conservative, and can be applied to $d_{50}/D>0.1$ (and not just to $0.1<d_{50}/D<0.2$), *but* may not lead to the minimum stone size for $d_{50}/D>0.2$.

The experimental results give some guidance in the choice of the safety factor, C_{SF}. The original (but revised for the range $0.2<d_{50}/D<0.4$) regression curves, i.e., with $C_{SF}=1$ for all ranges, are compared in Figures 4.7 through 4.9 with the corresponding curves with $C_{SF,I}=C_{SF,II}=1.2$, and $C_{SF,III}=1.5$. The least unstable

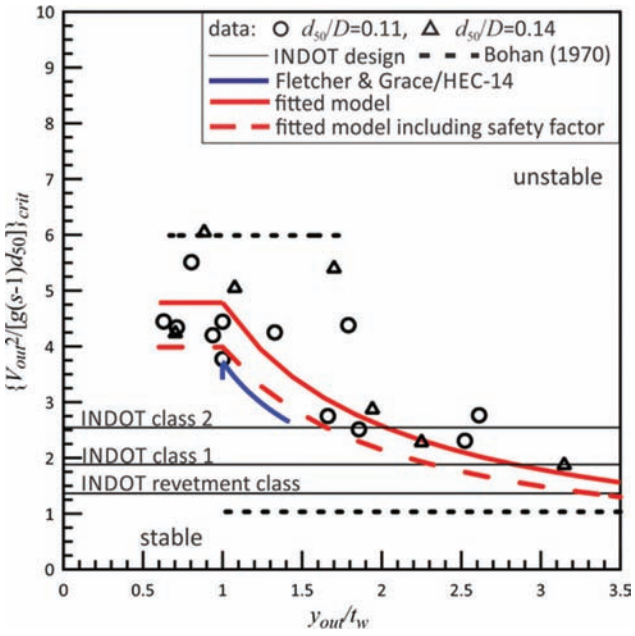

Figure 4.7 Comparison of the stability curves of different models, including the INDOT recommendations, with least unstable data points; the fitted model is that for $(d_{50})_I^*$, with $C_{SF,I}=1$ and 1.2, while the Bohan and HEC-14 models are evaluated for $d_{50}/D=0.11$.

data points, i.e., those with the lowest value of $V_{out}^2/[g(s-1)d_{50}]$, in each experimental series, are also plotted. A larger safety factor is applied to the curve based on the range $d_{50}/D>0.4$ due to the larger scatter and the fewer data points. Incorporating the safety factors displaces the respective curves so that they become located below all or almost all of the least unstable points. Included in Figure 4.7 through Figure 4.9 are also the corresponding curves for the current INDOT design, the Bohan, and the HEC-14 models for an appropriate d_{50}/D. More or less conservative choices of the safety factors may be made, depending on engineering judgment and project-specific circumstances. For example, in the application to be discussed in the next section, all safety factors were increased when applied outside the range, $0.66<y_{out}/t_w<3.5$, due to the very few data points outside of this range. In practice, an added safety factor is included in most cases because typically the next standard riprap class with a d_{50} larger than that given by the proposed design stone-sizing equations would be chosen.

Each of the proposed stone-sizing equations are restricted in their range of application. To simplify their application, a modified form that enforces the restriction may be expressed as

$$(d_{50})_I^* = \max\left\{\frac{C_{SF,I}}{4.78}\left[\frac{V_{out}^2}{g(s-1)}\right]\max\left[1,\left(\frac{y_{out}}{t_w}\right)^{0.89}\right],\ 0.1D\right\},$$

$$(d_{50})_{II}^* = \max\left\{\frac{C_{SF,II}}{6.58}\left[\frac{V_{out}^2}{g(s-1)}\right]\max\left[1.2,\left(\frac{y_{out}}{t_w}\right)^{0.86}\right],\ 0.2D\right\},$$

$$(d_{50})_{III}^* = \max\left\{\frac{C_{SF,III}}{6.10}\left[\frac{V_{out}^2}{g(s-1)}\right]\max\left[1,\left(\frac{y_{out}}{t_w}\right)^{0.5}\right],\ 0.4D\right\}.$$

(Eq. 4.8)

This form sets a minimum value for each equation, which is the minimum value for the applicability of Equation 4.7. In this formulation, each equation gives an adequate stone size for stability, and the minimum of the three values will therefore give the minimum adequate stone size for any specified condition. If the form in Equation 4.7 is used with the same value of C_{SF} for all three equations, then as noted earlier $(d_{50})_I$ will be largest as the most conservative, but the modified form in Equation 4.8 will not necessarily lead to $(d_{50})_I^*$ being the largest value. Setting a minimum value as in Equation 4.8 may lead to an overly conservative design for larger culverts ($D>6$ ft) at small design discharges, when V_{out} is small.

4.4.2 Procedures for Applying the Proposed Stone-Sizing Equations

Two procedures are outlined for applying the proposed stone-sizing equations (Equation 4.8). The first attempts to minimize the required computations, and might be appropriate for a manual or a "hand" calculation, while the second requires more computations but its logic is simpler, and so is suitable for a

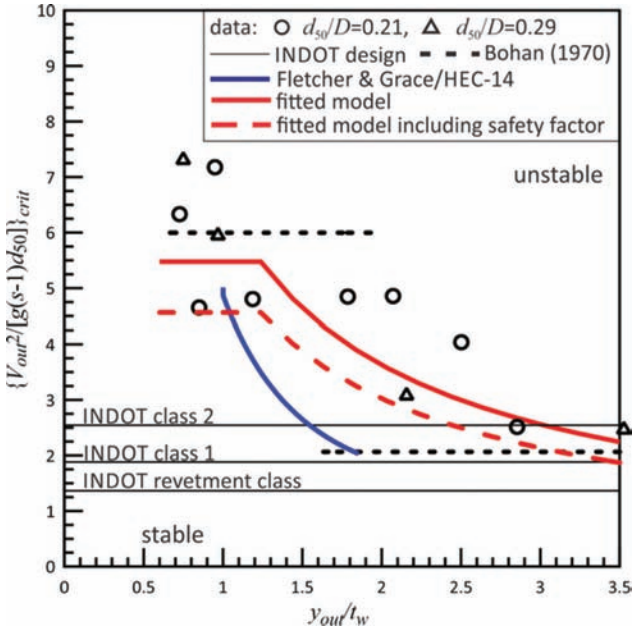

Figure 4.8 Comparison of the stability curves of different models, including the INDOT recommendations, with least unstable data points; the fitted model is that for $(d_{50})^*_{II}$, with $C_{SF,II}$=1 and 1.2, while the Bohan and HEC-14 models are evaluated for d_{50}/D=0.21.

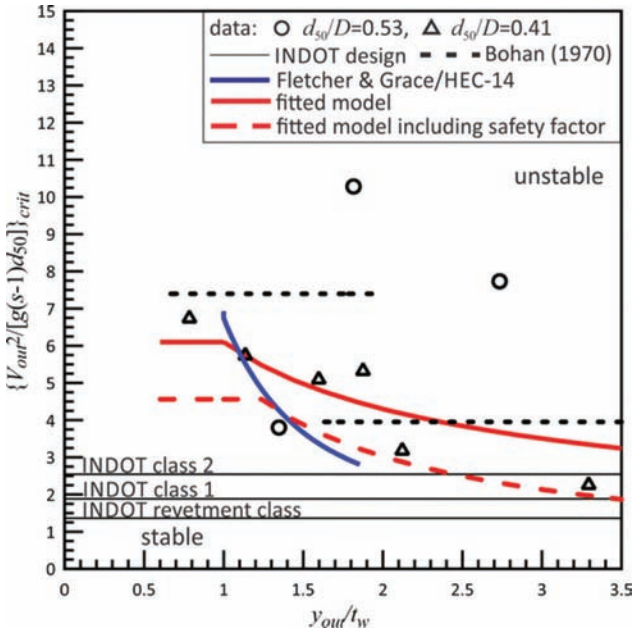

Figure 4.9 Comparison of the stability curves of different models, including the INDOT recommendations, with least unstable data points; the fitted model is that for $(d_{50})^*_{III}$, with $C_{SF,III}$=1 and 1.5, while the Bohan and HEC-14 models are evaluated for d_{50}/D=0.41.

spreadsheet solution. The first procedure evaluates the equations sequentially, and may be terminated early depending on whether a smaller stone size is possible or desired. A flow chart for the first procedure is given in Figure 4.10, and a step-by-step outline is given below. The second procedure always evaluates all three equations and then chooses the minimum of the three values, so more computational effort is required, but the final result is obtained without any complicated logic.

The steps in the first ("hand"-calculation) procedure may be listed as follows:

Step 1: Firstly, $(d_{50})^*_I$ is evaluated. If this is acceptable, e.g., if it already results in the smallest available riprap class, then the procedure is terminated, and $d_{50}=(d_{50})^*_I$ is chosen. In practice, the next standard riprap class with d_{50} larger than $(d_{50})^*_I$ would be chosen.

Step 2: If it is desired to check whether a stone size smaller than $(d_{50})^*_I$ might be adequate, it is checked whether $(d_{50})^*_I/D>0.2$ to see whether a smaller stone size might be possible, and if so, then $(d_{50})^*_{II}$ is evaluated. If this is acceptable, then the procedure is terminated with the choice, $d_{50}=(d_{50})^*_{II}$.

Step 3: If it is still desired to check whether a stone size smaller than $(d_{50})^*_{II}$ might be adequate, it is checked whether $(d_{50})^*_{II}/D>0.4$ to see whether a smaller stone size might be possible, and if so, then $(d_{50})^*_{III}$ is evaluated, and the procedure is terminated with the choice, $d_{50}=(d_{50})^*_{III}$.

The second procedure may be very briefly expressed as

$$d_{50} = \min\left[(d_{50})^*_I,(d_{50})^*_{II},(d_{50})^*_{III}\right],$$

so all three equations are evaluated, and the minimum value of the three is chosen as the minimum-stone-size solution.

Detailed numerical examples of applying the two procedures are given in Appendix A.

4.4.3 Applying the Proposed Stone Sizing Equations

The proposed stone-sizing equations were applied to a (not random) sample of 28 INDOT circular culverts along the I-70 freeway. Diameters ranged from 2 ft to 6.5 ft, though the large majority were larger than 3 ft and less than 6 ft. Outlet velocities ranged from 3.9 ft/s to 13.9 ft/s, with class 2 riprap being recommended by the current INDOT policy in 17 cases (≈ 60% of total cases). The tailwater levels relative to the diameter, t_w/D, ranged from 0.2 to 2, while y_{out}/t_w ranged from 0.5 to 4.3. More than half of the cases featured supercritical flow within the culvert. All data were taken from HY-8 files provided by INDOT personnel. In the analysis, a safety factor, C_{SF}=1.2, was applied in the computation of $(d_{50})^*_I$ and $(d_{50})^*_{II}$ for the range, $0.66<y_{out}/t_w<3.5$, but this was increased to C_{SF}=1.5 outside this range due to the relative sparsity of data. The safety factor was similarly chosen as previously recommended C_{SF}=1.5 in the computation of $(d_{50})^*_{III}$ in the range, $0.66<y_{out}/t_w<3.5$, and increased to C_{SF}=2 outside this range. Detailed input data and results are given in Figure 4.11, which also provides a comparison with the results using the current INDOT design policy, the HEC-14 and the Bohan models. The second procedure (from the preceding subsection) was applied as being simpler to implement in a spreadsheet solution.

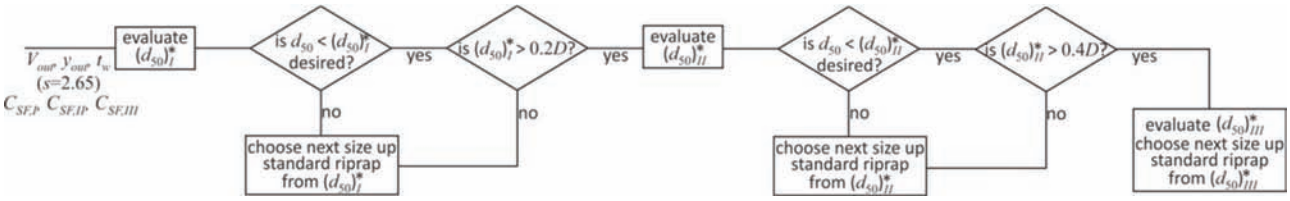

Figure 4.10 Flowchart for the logic of the manual ("hand") computation procedure.

From Figure 4.11, in 21 of the 28 cases considered, i.e., 75% of cases, the proposed stone-sizing procedure would support a smaller standard INDOT riprap class being chosen compared to the current INDOT design policy. This should not be too surprising as the previous comparisons of the various models have indicated that the current INDOT design policy is conservative compared to the proposed stone-sizing equations. In the large majority of such cases, the next smaller class is found adequate, but in isolated cases, a riprap class two steps smaller (e.g., from dissipator being required to a class 1 riprap) is deemed adequate. In the large majority of cases, $d_{50}=(d_{50})^*_I$, is ultimately chosen, likely because in this sample most cases involved diameters 4 ft and larger. Further, although the computational safety factor applied in almost all cases was 1.2 (because either $(d_{50})^*_I$ or $(d_{50})^*_{II}$ was ultimately chosen), the actual safety factor due to the fact that in practice the next larger riprap class is chosen often exceeded 1.5. Somewhat unexpected, in two cases, the proposed procedure leads to a riprap "class" (dissipator) that is *larger* and hence is more conservative than that (class 2) recommended by the current INDOT policy. In both cases, this is attributed to the low values specified for t_w, which led to large values of $y_{out}/t_w \approx 4$, and hence to large required stone sizes. This highlights the importance of the specification of tailwater conditions for the proposed procedure. In both cases, where a larger required riprap class was found by the proposed procedure, t_w was simply specified in HY-8 as 1 ft, which may have been an arbitrary value not necessarily reflective of actual design conditions, possibly chosen as being irrelevant to predictions of culvert performance. Thus, greater care will be needed in specifying t_w in the proposed procedure.

The predictions of the two other main models (the HEC-14 and the Bohan models) are also given in Figure 4.11. As noted earlier, HEC-14 recommends that the model be restricted in application to the range, $0.4<t_w/D<1$, which as seen in Figure 4.11 may be rather limiting as $\approx$ 50% of the cases fall outside of this range (in Figure 4.11, a blank cell is given if the HEC-14 model is not applicable). Within the restricted range, the minimum stable stone size according to the HEC-14 model is generally but not always larger than that by the proposed equations with the recommended safety factors used (and the minimum pipe sizes set). The maximum difference (with the HEC-14 value being 55% larger) between the two models is not large, but ultimately only three (of the fourteen where the HEC-14 model is applicable) cases lead to a different INDOT riprap class because the small differences are not sufficiently large as to cause a move to the next larger riprap class.

The Bohan model is not as restricted in its application as the HEC-14 model, but in at least one instance of a low-discharge maximum-tailwater case, a negative value is obtained from the Bohan equation, which is clearly non-physical and unacceptable (also represented as a blank cell). Compared to the proposed model, the Bohan required stone size is much more erratic, due to the step-like change between a more conservative minimum-tailwater size and a less conservative maximum-tailwater size. Thus, Bohan required stone size ranges in value from 26% to over 300% of the proposed required stone size. This large variability has the practical consequence that the Bohan model prescribes in eight (of 28) cases a next *larger* INDOT riprap class and also in another 8 cases a next *smaller* INDOT riprap class than the proposed model. It is also noteworthy that, in two of the three cases where the recommendations of the proposed equations differ from those of the HEC-14 model, the recommendations agree with the Bohan model.

The above results by themselves demonstrate only that the application of the proposed equations will often lead to the choice of riprap class smaller than that following the current INDOT policy, and does not indicate whether the recommendations are reliable. Nevertheless, that the recommendations largely agree with the other main models (when the latter are applicable) does give assurance that the recommendations can be relied on. It should also be emphasized that the stone-sizing equations give a *minimum* required stone size and by extension riprap class, but engineering judgment must still be exercised in deciding whether this minimum is the most appropriate solution for any given problem.

4.4.4 Limitations and Broader Applications of the Proposed Stone Sizing Equations

As they are based on experiments, the proposed stone-sizing equations (Equation 4.8) are expected to be most reliable when applied within the range of conditions on which they were based. The experiments were performed with nearly horizontal smooth circular pipes with subcritical or full-pipe flow in the pipe. Such or similar conditions also characterized the earlier studies, such as Bohan (1970), that formed the basis of the Bohan and the HEC-14 models. The parameters, d_{50}/D ranged from 0.1 to 1.5, y_{out}/t_w from 0.6 to 4, and $V^2_{out}/[g(s-1)d_{50}]$ from 0.1 to 15 (see also Table 3.1), and caution is needed if the equations are to be applied in a range that is drastically different.

EXCEL worksheet for proposed stone-sizing equations

		INDOT riprap	assumed d_{50} (ft)
		revetment:	0.58
g=	32.2 ft/s^2	class 1:	1
specific gravity, s=	2.65	class 2:	1.25

regression constants	I	II	III
a=	4.78	6.57	6.10
b=	0.89	0.86	0.50

assumed C_{SF} values	I	II	III
default	1.2	1.2	1.5
alternate	1.5	1.5	2

yellow highlight: cases where the proposed equations lead to a smaller minimum recommended standard riprap class than the current INDOT guidelines
red highlight: cases where the proposed equations lead to a design more conservative than the current INDOT guidelines
gray highlight: cases done in the example calculations in the Appendix
Where cells are blank, either the result is unphysical or the given conditions are outside of the recommended range of application of model.

	Data from HY-8 files						proposed stone-sizing equations											INDOT design	HEC-14 model		Bohan model	
Structure ID	diameter, D	discharge, Q	tailwater depth, t_w	outlet velocity, V_{out}	y_{out}	flow regime	y_{out}/t_w	$V_{out}^2/[g(s-1)]$	$C_{SF,I}$	$(d_{50})_I^*$	$C_{SF,II}$	$(d_{50})_{II}^*$	$C_{SF,III}$	$(d_{50})_{III}^*$	min. d_{50}	INDOT riprap class			d_{50}	riprap class	d_{50}	riprap class
	(ft)	(cfs)	(ft)	(ft/s)	(ft)			(ft)		(ft)		(ft)		(ft)	(ft)				(ft)		(ft)	
70srt01	5	164.4	4.74	8.54	4.74	Sub	1.00	1.37	1.20	0.500	1.20	1.000	1.50	2.000	0.500	revetment		class 1	0.44	revetment	0.09	revetment
70str03	4	107.7	2.57	10.19	3.12	Super	1.21	1.95	1.20	0.583	1.20	0.800	1.50	1.600	0.583	class 1		class 2	0.71	class 1	0.30	revetment
70str04	4	124.3	2.58	12.43	2.88	Super	1.12	2.91	1.20	0.805	1.20	0.800	1.50	1.600	0.800	class 1		class 2	0.90	class 1	0.50	revetment
70srtr05	5.5	653.8	11.09	12.42	5.50	Sub	0.50	2.90	1.50	0.911	1.50	1.100	2.00	2.200	0.911	class 1		class 2			0.46	revetment
70str06	5	99.8	2.08	8.7	2.84	Super	1.37	1.42	1.20	0.500	1.20	1.000	1.50	2.000	0.500	revetment		class 1	0.74	class 1	0.86	class 1
70str07	5.5	78.2	2.41	9.45	2.08	Sub	0.86	1.68	1.20	0.550	1.20	1.100	1.50	2.200	0.550	revetment		class 1	0.46	revetment	0.98	class 1
70str08	5	288.2	4.36	13.91	4.47	Super	1.03	3.64	1.20	0.935	1.20	1.000	1.50	2.000	0.935	class 1		dissipator	1.01	class 2	0.62	class 1
70str12	5.5	166.3	1.93	10.79	3.30	Super	1.71	2.19	1.20	0.887	1.20	1.100	1.50	2.200	0.887	class 1		class 2			1.11	class 2
70str13	5	161.9	3.95	9.75	3.95	Sub	1.00	1.79	1.20	0.500	1.20	1.000	1.50	2.000	0.500	revetment		class 1	0.52	revetment	0.21	revetment
70str14	4.5	137.6	1.51	12.99	2.77	Super	1.83	3.18	1.20	1.368	1.20	0.977	1.50	1.800	0.977	class 1		class 2			1.21	class 2
70str14a	4.5	36.7	0.99	9.2	1.31	Super	1.32	1.59	1.20	0.513	1.20	0.900	1.50	1.800	0.513	revetment		class 1			0.86	class 1
70str16	5	269.1	4.95	12.8	4.95	Super	1.00	3.08	1.20	0.774	1.20	1.000	1.50	2.000	0.774	class 1		class 2	0.81	class 1	0.51	revetment
70str17	4	150.9	3.63	10.63	3.63	Sub	1.00	2.13	1.20	0.534	1.20	0.800	1.50	1.600	0.534	revetment		class 2	0.69	class 1	0.34	revetment
70str19	4	49.4	1.98	7.36	2.11	Sub	1.07	1.02	1.20	0.400	1.20	0.800	1.50	1.600	0.400	revetment		class 1	0.28	revetment	0.65	class 1
70str20	4	24.4	0.99	7.9	1.14	Super	1.15	1.17	1.20	0.400	1.20	0.800	1.50	1.600	0.400	revetment		class 1			0.70	class 1
70str22	4	69.4	1.5	10.82	2.05	Super	1.37	2.20	1.20	0.730	1.20	0.800	1.50	1.600	0.730	class 1		class 2			0.95	class 1
70str24	5.5	182.9	1.46	10.49	3.78	Sub	2.59	2.07	1.20	1.212	1.20	1.100	1.50	2.200	1.100	class 2		class 2			1.08	class 2
70str25	6.5	161.9	1.55	9.92	3.13	Sub	2.02	1.85	1.20	0.869	1.20	1.300	1.50	2.600	0.869	class 1		class 1			1.11	class 2
70str27	4.5	228.1	1	12.77	4.27	Super	4.27	3.07	1.50	3.506	1.50	2.442	2.00	2.079	2.079	dissipator		class 2			1.26	dissipator
70str28	5	238.8	4.25	13.17	4.35	Super	1.02	3.26	1.20	0.837	1.20	1.000	1.50	2.000	0.837	class 1		class 2	0.81	class 1	0.55	revetment
70str29	4	124.4	1	11.07	3.35	Super	3.35	2.31	1.20	1.698	1.20	1.192	1.50	1.600	1.192	class 2		class 2			0.98	class 1
70str30	5	253.8	1	11.35	3.92	Super	3.92	2.42	1.50	2.566	1.50	1.792	2.00	2.000	1.792	dissipator		class 2			1.12	class 2
70str32	4	108.7	1	10.23	3.15	Super	3.15	1.97	1.20	1.373	1.20	0.965	1.50	1.600	0.965	class 1		class 2			0.90	class 1
74str03	3	66.5	1.78	10.36	2.61	Super	1.47	2.02	1.20	0.713	1.20	0.600	1.50	1.200	0.600	class 1		class 2	0.77	class 1	0.34	revetment
74str21	2.5	18.9	1.81	4.97	1.81	Sub	1.00	0.46	1.20	0.250	1.20	0.500	1.50	1.000	0.250	revetment		revetment	0.16	revetment		
74str22	3	83.6	3.46	10.29	3.00	Super	0.87	1.99	1.20	0.500	1.20	0.600	1.50	1.200	0.500	revetment		class 2			0.34	revetment
74str36	2	3.6	0.67	3.9	0.67	Sub	1.00	0.29	1.20	0.200	1.20	0.400	1.50	0.800	0.200	revetment		revetment			0.24	revetment
74str42	2.5	43.1	1.88	9.44	2.19	Super	1.16	1.68	1.20	0.482	1.20	0.500	1.50	1.000	0.482	revetment		class 1	0.47	revetment	0.28	revetment
maximum:	6.5	653.8	11.09	13.91	5.5		4.27	3.64														
minimum:	2	3.6	0.67	3.9	0.67		0.50	0.29														

Notes:

- The flow regime within the culvert is denoted as "Sub" for subcritical, and "Super" for supercritical.
- The safety factor for each equation is chosen as discussed in the text, except that larger values are used in the range where data are sparse.
- For choosing the standard INDOT riprap classes, it is assumed that d_{50} = 0.58 ft, 1 ft, and 1.25 ft for revetment, class 1, and class 2 riprap respectively.

Figure 4.11 Detailed numerical values used in EXCEL spreadsheet for the application of stone-sizing computations.

The equations are however expected to be relatively robust for some conditions different from the experiments. As argued in Chapter 2, the formulation in terms of V_{out} and y_{out} rather than Q (as in the HEC-14 model) should make the equations still roughly applicable to flows supercritical in the pipe. Except for the cases with the smallest stone, in the majority of data points, the outlet Froude number, $V_{out}/\sqrt{gD}$, exceeded 1, and in some points with the largest stone and smaller pipe, exceeded 5, but these were generally full-pipe flows and so might not be considered supercritical flows in the strict sense. Of most concern but also least common, certainly in an Indiana context, would be an extreme situation where the y_{out}/D is small and t_w/D is large. In the more common case, where y_{out} is comparable to D, and t_w is comparable to or less than y_{out}, the proposed equations should be applicable, though an increased safety factor may be considered. A number of the cases in Figure 4.11 were supercritical, but in none of them did $V_{out}/\sqrt{gy_{out}}$ exceed 1.5 or at the same time $y_{out}/D<0.5$ and $y_{out}/t_w<1$.

Similarly, applications to the much rougher corrugated metal pipe (CMP) should also present no problem (in HEC-14, examples are given in which the HEC-14 model is applied to CMP without any special treatment). The main difference with a rough pipe (at the same V_{out} and y_{out}) would be the higher turbulence level due to the larger roughness elements, which might affect the stone mobilization as larger fluctuations from the mean could enhance mobilization at the same mean $V_{out}^2/[g(s-1)d_{50}]$. In practice, the higher flow resistance in a CMP would be expected to result in relatively low outlet velocities, so that even if a somewhat increased safety factor is applied the resulting minimum adequate stone size would still remain reasonable.

Application to non-circular culvert geometries is also of interest (though less so for smaller culverts), but requires careful consideration. Again the model formulation in terms of V_{out} and y_{out} are definite advantages, but the proposed equations also involve d_{50}/D and the minimum for each equation is a fraction of D, so it is necessary to find the most appropriate substitute for D. One option for an equivalent diameter, D_{eq}, may be based on the equality of areas as in HEC-14. For example, for a box culvert, this would imply $D_{eq}=\sqrt{WH/(\pi/4)}$, where W is the span and H the rise. Alternatively, D_{eq} could be chosen as either the span or the rise. If the rise and span are comparable in magnitude, e.g., a square box culvert, then both options will yield similar results, and with the uncertainty in the proposed equations, either could be used without significant differences in the final choice of d_{50}. In some applications, spans may be quite larger than rises, and the different choices of D_{eq} may affect the result for d_{50}. As a type of geometric mean, the area-based D_{eq} may be still be appropriate though its physical basis is at best tenuous. It may be argued that the main effect due d_{50}/D not already captured in y_{out}/t_w is the lateral extent of the apron that is subjected to the outflow. From this perspective, the span might be argued as the more physically based choice for D_{eq}. If the span is larger than rise, as is more usually the case, then this choice would also be the more conservative, though as pointed out earlier, for larger spans (>6 ft) and low design discharges, this might be overly conservative.

The proposed equations were aimed primarily at smaller culverts ($D_{eq}\leq$6 ft) for which a simple riprap apron would be the most common outlet protection. They should be applicable for larger structures, but as noted is likely to be overly conservative for small design discharges, due to the minimum of $0.1D_{eq}$ that is set. While such a constraint is not practically important if D_{eq}=4 ft, it becomes of concern if D_{eq}=12 ft, as the latter would require class 2 riprap for even small discharges. While experiments were limited to $d_{50}/D<0.53$, this does not necessarily place a lower limit of application in terms of D_{eq}. The experimental results indicate that, as d_{50}/D increases, the stability requirements become less stringent, so that the equations developed with data for which $d_{50}/D<0.53$ should be applicable to $d_{50}/D>0.53$ though may not necessarily lead to a minimum-stone-size solution.

4.5 Point Velocity Measurements

While apron-length (and width) sizing was not studied directly in a manner similar to stone sizing, it was examined indirectly in two ways. Firstly, point velocities immediately downstream of the outlet were measured in order to assess the extent to which the outlet velocity was reduced or dissipated in the presence of a relatively rough apron surface. Secondly, some limited experiments were conducted, with a short section of sand bed downstream of the model riprap apron, to examine the conditions under which noticeable scour occurred downstream of the apron.

Velocity measurements were obtained in four experiments with the same pipe diameter (D=0.35 ft). In three experiments, the riprap apron consisted of stones with d_{50}=2.24 in (so that d_{50}/D=0.53), while in the fourth experiment, the bed was essentially smooth (the surface was a HDPE plastic, with an estimated Manning's n of 0.011). Two tailwater (T) levels and two discharges (Q) were investigated. For ease of referencing, the four experiments are labelled as QLTLR (low Q, low T, rough-bed), QLTHR (low Q, high T, rough-bed), QHTLR (high Q, low T, rough-bed), and QHTLS (high Q, low T, smooth-bed). Transverse (across the channel) profiles were obtained at a single elevation at approximately the tailwater mid-depth, at four streamwise sections up to x/D=8.9, where x is the streamwise distance from the outlet. It is recalled that INDOT design policy specifies only a minimum apron length of 4D, while HEC-14 recommends an apron length varying with stone size with however a maximum of 8D. For this set of experiments, x/D=8.9 is approximately the end of the model riprap apron, and the start of the end sill. Figure 4.12 examines the effect of tailwater depth by comparing the velocity profiles with nominally the same (low)

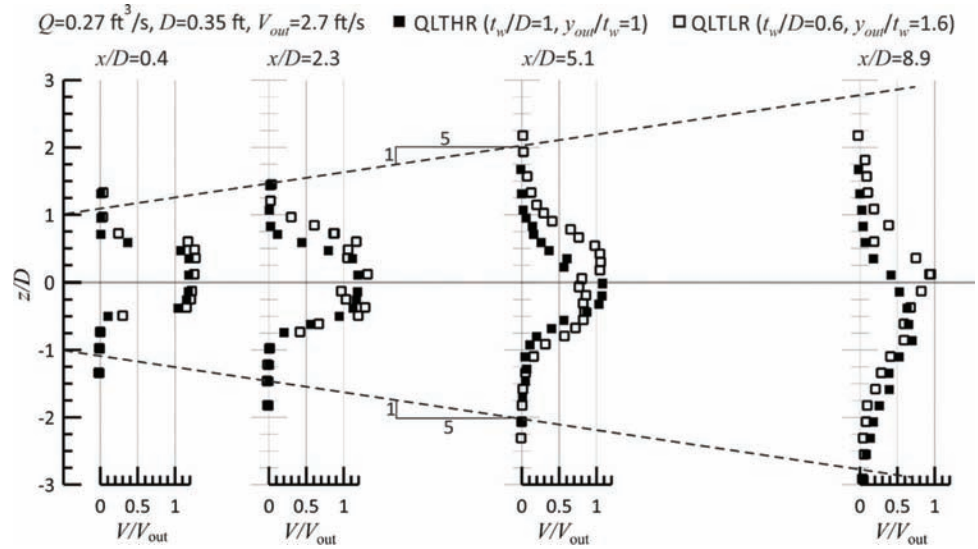

Figure 4.12 Comparison of normalized transverse (across the channel) point velocity profiles at different channel sections (different distances, x/D, downstream of the outlet) for the same nominal discharge but different tailwater levels (■ – high tailwater ($t_w/D=1$), □ – low tailwater ($t_w/D=0.6$).

discharge but different tailwater depths. In both low and high tailwater cases, the pipe flowed full throughout so that V_{out} is the full-flow average pipe velocity. This bears mention as HY-8 predicts, for the low-discharge case, an outlet depth at the pipe critical-flow depth which is $\approx 0.8D$, and hence an actual outlet velocity that is $\approx$ 10% higher than V_{out}. Very near the outlet ($x/D=0.4$), in both cases, the maximum measured point velocity, $V_{\max}$, exceeds V_{out} by $\approx$ 18% in the case of QLTHR and $\approx$ 27% in the case of QLTLR. As a result, even by $x/D=5.1$, i.e., farther than the minimum INDOT design apron length, $V_{\max}/V_{out}>1$. As $t_w/D>0.5$ in the low-tailwater case, it does not technically qualify as a minimum-tailwater case in the Bohan sense.

The effect of tailwater on the velocity is not dramatic, but initially (at least up to $x/D=2.3$) $V_{\max}/V_{out}$ is slightly but consistently larger in the low-tailwater case. This is mainly attributed to the conversion of piezometric to kinetic energy as the outflow plunges into the low-tailwater channel. The profile of V/V_{out} tends to be broader for QLHLR, consistent with the Bohan model, which prescribes a wider apron for the minimum-tailwater case. Also drawn in Figure 4.12 are dashed lines reflective of a 1:5 apron-width flaring, showing that the outflow jet is contained well within 1:5 flaring even up to $x/D=8.9$. Technically, both of these cases fall within the maximum-tailwater case of Bohan ($t_w/D>0.5$), so the Bohan prescription of a 1:5 width flaring could be justified. Nevertheless, the low-tailwater ($t_w/D=0.6$) profile suggests that the INDOT recommended 1:4 flaring is likely adequate even for $t_w/D<0.5$. At the most downstream section, $V_{\max}/V_{out}$ in QLTLR remains quite large compared to QLTHR, indicating that energy dissipation is larger for high-tailwater conditions. Noticeable also is that, as noted earlier, under high-tailwater conditions, the outflow jet has more of a tendency to migrate from the channel centerline, such that $V_{\max}/V_{out}$ is observed at a location distinctly away from the centerline.

Because the low-tailwater case generally requires the larger stone size, the remaining cases in which velocity profiles were measured were restricted to this case. The effect of an increased discharge under low-tailwater conditions may be seen in Figure 4.13. As might be expected, the differences between QLTLR and QHTLR are somewhat less than in the previous comparison of QLTHR and QLTLR, and so the previous comments on QLTLR are generally applicable also to QHTLR. One aspect of the high-discharge case should be pointed out: the higher the discharge (or $Q/\sqrt{gD^5}$ or $V_{out}/\sqrt{gD}$) the more horizontal the trajectory of jet discharge from the outlet, and the farther downstream that this jet fully enters the tailwater. This likely explains the main differences seen in the profiles for QLTLR and QHTLR at $x/D=2.3$ and 5.1, and to a lesser extent $x/D=8.9$

Figure 4.14 examines more directly the effect of roughness (for the same tailwater and discharge) as profiles with a riprap apron (QHTLR) and with a smooth bed (QHTLS) are compared. Differences are more pronounced, especially in view of the almost identical starting profiles at $x/D=0.4$. The jet width at $x/D=2.3$ and 5.1 is broader with QHTLR than with QHTLS, with the consequence of a larger $V_{\max}/V_{out}$ observed most clearly at $x/D=5.1$. Thus, the large roughness of the apron riprap does result in a measurable increased dissipation and reduced maximum velocities of the outlet jet, which however may be insufficient under practical conditions to avoid scour occurring downstream of relatively short ($L_a/D\leq 5$) aprons. Also very noticeable is the substantial migration of the jet under smooth-bed condition away from the channel centerline, which was always minor under low-tailwater conditions and even less under high-tailwater conditions.

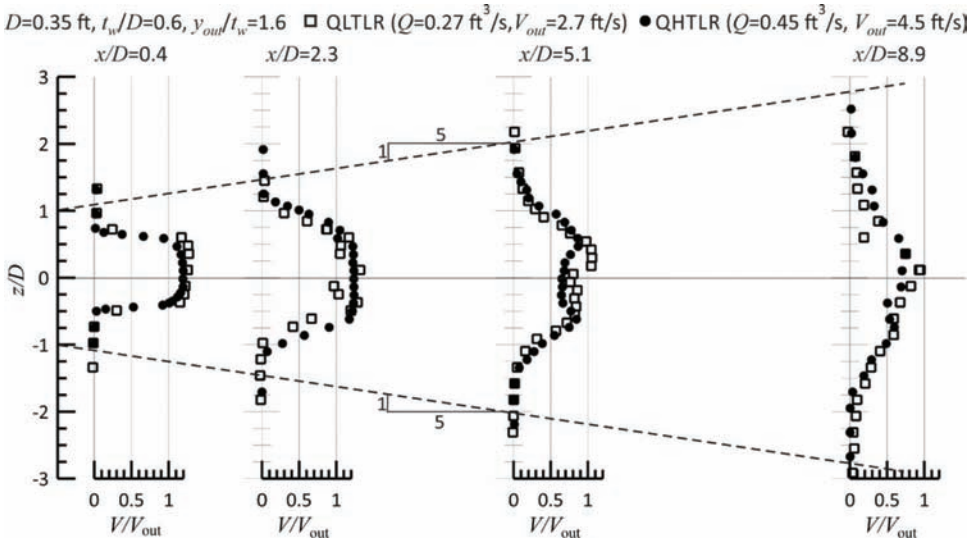

Figure 4.13 Comparison of normalized transverse (across the channel) point velocity profiles at different channel sections (different distances, x/D, downstream of the outlet) for the same nominal low-tailwater (t_w/D=0.6) level but different discharges (□ – low discharge, Q=0.27 ft^3/s, ● – high discharge, Q=0.45 ft^3/s).

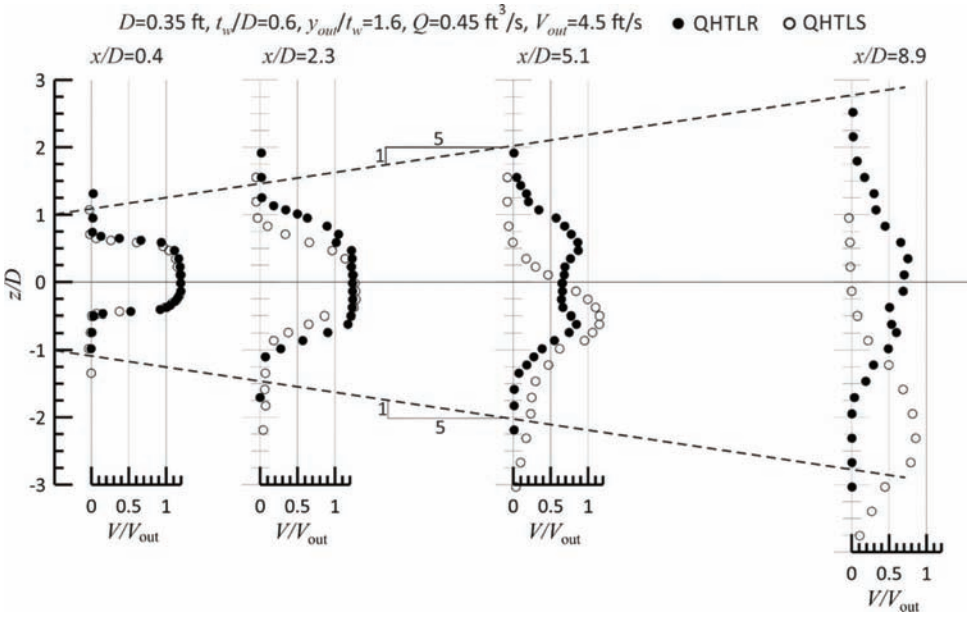

Figure 4.14 Comparison of normalized transverse (across the channel) point velocity profiles at different channel sections (different distances, x/D, downstream of the outlet) for the same nominal low-tailwater (t_w/D=0.6) level and discharge (Q= 0.45 ft^3/s), but with different bed condition (○ – smooth bed, ● riprap apron, d_{50}=2.2 in or d_{50}/D=0.53).

The variation of V_{max} with downstream distance is summarized in Figure 4.15, plotted with different normalizations. The first normalization in Figure 4.15a uses the maximum (point) velocity at the outlet, $(V_{max})_{out}$, and allows comparison with the reference curve given in Figure 2.7 (given in both HEC-14 and the INDOT Design Manual), though Figure 4.15a prefers linear rather than logarithmic axes. There is general agreement with the reference curves, and the magnitude of the deviations from the curve are similar to those found in the data points of Figure 2.7. Because $(V_{max})_{out}$ is not easily available, a more practically useful normalization uses the average full-flow outlet velocity, V_{out}, i.e., the same used in Figure 4.12 through Figure 4.14. Thus, by x/D=5.1, the lowest observed V_{max} is still over 80% of V_{out} and by x/D=8.9 is still only ≈ 70% of V_{out}. As an example, if these values are applied to a case with V_{out}=11 ft/s so that according to the current INDOT design policy class 2 riprap would be chosen for the apron, then even if the apron 8 D is long, the velocities immediately downstream of the apron would exceed 7 ft/s and so would require class 1 riprap

downstream of the class 2 riprap in order to avoid downstream scour.

4.6 Scour Downstream of Apron

The possibility of scour downstream of the riprap apron was studied in a limited number of experiments in which a short (≈ 0.67 ft) section of coarse sand (d_{50}≈1.7 mm) was installed downstream of the model apron, separated by a 1/8-in thick aluminum divider located ≈ 7D downstream of the outlet. These experiments were conducted with only the smallest stone (d_{50}≈0.61 in) and with flow from only the 5.75-in pipe. Images after two such experiments are shown in Figure 4.16. The aftermath of a relatively high-tailwater case (t_w/D=0.57, y_{out}/t_w ≈1) is shown in Figure 4.16a. Despite the flow corresponding to a stable apron ($V_{out}^2/[g(s-1)]$=2.6), and an apron length of ≈7D, a scour hole reaching the underlying false floor has developed in the coarse-sand section. In contrast, Figure 4.16b shows the situation after a low-tailwater case (t_w/D=0.26, y_{out}/t_w ≈2.7) where the apron has suffered catastrophic failure (numerous stones mobilized from the upstream apron can be seen deposited in the coarse-sand section, and $V_{out}^2/[g(s-1)]$=3.5). While it is evident that the coarse sand has been eroded and has deposited in the end-sill section, there was no deep scour hole as was seen in the high-tailwater case of Figure 4.16a even though the value of $V_{out}^2/[g(s-1)]$ was larger. The difference in scour behavior is attributed to the more concentrated high-speed flow in the high-tailwater case leading to a deep scour hole, while in the low-tailwater case, the jet flow tended to be more diffuse as seen in the transverse velocity profiles leading to moderate erosion over a larger region but no deep scour hole. It may be mentioned however that, in this low-tailwater case, sand was already observed in the end-sill section and hence already being eroded even when the apron was stable.

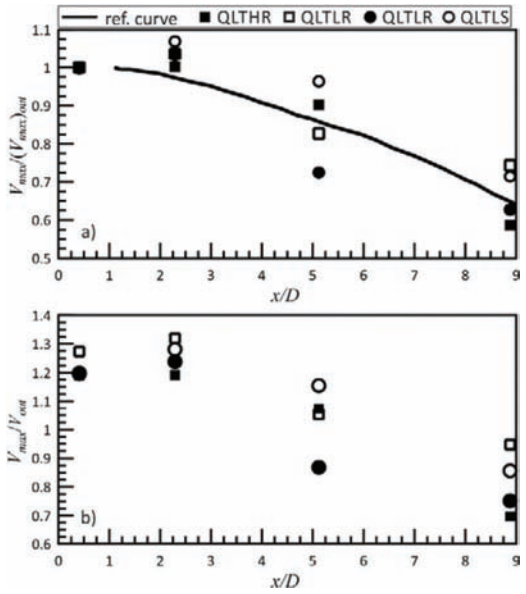

Figure 4.15 Variation of normalized maximum measured point velocity, V_{max}, with normalized distance, x/D, downstream of the outlet, (a) normalization with the maximum measured point velocity at the outlet, $(V_{max})_{out}$, (b) normalization with the average outlet velocity, $V_{out}=Q/(\pi D^2/4)$.

4.7 Summary

The experimental data, grouped according to narrow ranges of the stone size relative to the pipe diameter, d_{50}/D, were sorted into different stability categories, based on the number of mobilization events observed during a video record lasting at least 10 minutes for given apron, tailwater, and flow characteristics. Using a definition of instability as more than one mobilization event, logistic regression was applied to determine a "best"-fit curve to separate stable and unstable conditions. Stone-sizing equations, including safety factors, were then constructed from the "best"-fit curve, and a procedure for obtaining a minimum required stone size was developed. In a test of the proposed stone-sizing equations, the procedure was applied to a sample of actual culverts, and was found to yield smaller standard INDOT riprap classes in a large majority of cases, though could lead to larger riprap classes for problems with sufficiently low tailwater depths.

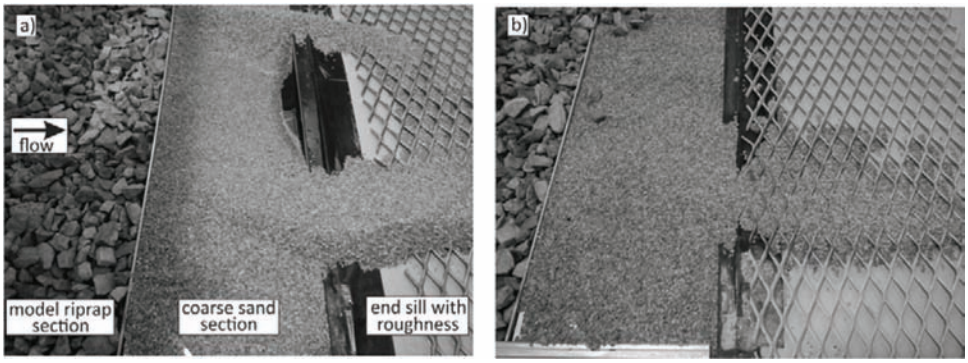

Figure 4.16 Photographic images taken after downstream-scour experiments: (a) higher-tailwater but stable-apron conditions with substantial downstream scour, (b) lower-tailwater but catastrophic-failure apron conditions with only moderate downstream scour.

Transverse point-velocity profiles were measured at streamwise distances up to approximately 9 pipe diameters downstream of the outlet in order to study the effects of tailwater depth, increased discharge, and especially stone roughness on the degree to which velocity is reduced by the apron, with implications for scour downstream of the apron. A notable effect of roughness was observed in the profiles, but the degree to which the velocity is reduced by the end of the apron is believed to be insufficient to avoid downstream scour. Downstream scour even when the apron was stable was also observed, and may be especially severe for high tailwater conditions when the apron could be stable even with relatively large outlet velocities.

5. SUMMARY, CONCLUSIONS, AND RECOMMENDATIONS

The present study investigated primarily the appropriate stone-sizing of riprap aprons, and more specifically whether the current INDOT design policy based solely on outlet velocity may be overly conservative especially within the context of smaller culverts. In the literature review, two alternative stone-sizing equations were identified, that due to Bohan (1970) and that due to Fletcher and Grace (1972), both of which have been adopted by numerous state agencies in some form (the Fletcher and Grace model with some adjustments being recommended in HEC-14). The various models were discussed in terms of a synthesis or framework equation, motivated by riprap-design models for streambank stabilization. Experiments were performed in the laboratory with two pipe sizes, 4.25 in (0.35 ft) and 5.75 in (0.48 ft), and four stone sizes, median diameters estimated to be d_{50}=0.61 in, 1.22 in, 1.73 in, and 2.24 in, for a range of discharges and tailwater depths.

The experimental results from video recording of the flow over a laboratory stone apron provided the empirical basis for proposed stone-sizing equations and procedure. Scores were assigned to each case based on visual detection of mobilization events, and stable and unstable cases were distinguished based on the number of independent mobilization events identified in the video record. The data were then sorted into three ranges of d_{50}/D, and logistic regression applied to determine three stone-sizing equations involving not only outlet velocity (as the current INDOT design policy), but also tailwater depths and culvert diameters. The equations were modified so that they were ordered in that each was more conservative than the next, and thus applicable not only to the data (d_{50}/D) range on which it was based, but also to larger d_{50}/D range. Further, a safety factor was introduced, and a minimum size was set to be consistent with the range of application of each equation. Two procedures were described for using the proposed equations, one aimed for a manual (or "hand") computation, and the other aimed for a computer (e.g., spreadsheet) solution.

In comparison to the current INDOT design policy, the proposed approach typically but not always predicts a smaller minimum stone size required for apron stability. In an application to a sample of 28 actual culverts, with data from HY-8 results, the proposed approach, including the recommended safety factor, was found to lead to a smaller required standard INDOT riprap class in 75% of cases. The proposed approach can however in cases of low relative tailwater depths lead to recommended riprap classes more conservative than the current INDOT policy, and greater care in specifying the tailwater conditions may be needed if the proposed procedure is adopted. Compared to the HEC-14 model, the proposed approach has the advantage of being applicable over a broader range of tailwater depths, as the HEC-14 approach was found to be inapplicable to $\approx$ 50% of cases. Although the proposed approach yielded smaller values of minimum stone-size diameter compared to the HEC-14 model, for the applications to the sample of actual culverts, it recommended a smaller standard INDOT riprap class in only 3 of 14 cases for which the HEC-14 model was applicable. The recommendations of the Bohan model were more erratic, attributed to its maximum-tailwater equation being too lax, and its minimum-tailwater equation being generally too conservative.

A secondary aim of the study was an examination of the velocity field downstream of the outlet, and the possible implications for scour downstream of the apron. Point velocity measurements were obtained for four cases, all with the same 4.25-in diameter pipe, three of which involved the largest (d_{50}=2.2 in) stone, and one over a smooth bed. In the three cases with a stone apron, the apron extended a distance of $\approx$ 9 pipe diameters downstream of the outlet. In all cases, substantial velocities (maximum velocities greater than 70% of than the average outlet velocity) were observed at distances beyond distances typically recommended for the lengths of riprap apron. The observed lateral extent of the outlet jet flow was narrower than expected, and suggests that a minimum 1:4 (the current INDOT design guideline) or even a 1:5 apron flaring would be adequate in most cases. The main qualification relates to a possible migration of the entire jet flow away from the culvert centerline for certain conditions, so that, even though the jet itself remains narrow, its location can be quite uncertainty. A comparison between rough-bed and smooth-bed results indicated a measurable reduction in maximum velocity due to the rough apron, but this reduction is still likely insufficient to prevent scour downstream of the apron in most practical cases (depending on streambed substrate) even if the apron extends to 9 pipe diameters (let alone 4 pipe diameters, the current INDOT recommended minimum apron length). Results from some limited experiments with a short coarse sand-bed section downstream of the laboratory stone apron suggest that the more concentrated jet flow under high-tailwater conditions may lead to greater downstream scour than the more diffuse jet flow under low-tailwater conditions.

The proposed stone-sizing equations and procedure may be recommended for estimating the minimum required stone size for stable aprons for culvert outlets when tailwater depths can be reliably estimated. For moderate values of the ratio of outlet depth to tailwater depth, say <2, the proposed procedure will generally lead to a recommended standard riprap class smaller than the current INDOT policy. While applicable to larger structures, it may be overly conservative if small design discharges are involved, due to a minimum pipe size being incorporated in the equations. Although their formulation in terms of an outlet velocity and an outlet depth and the general conservatism in their development should make the proposed equations relatively robust, their application to cases very different from the experimental basis should be considered with the appropriate caution and probably with increased safety factors. Velocity measurements indicating that potentially scour-inducing velocities still remain at sections downstream of apron lengths such as those recommended in INDOT design guidelines as well as in HEC-14 suggest that the INDOT apron-length guidelines may need re-examination.

REFERENCES

Berry, N. K. (1948). *The start of bed-load movement and the relation between competent bottom velocities in a channel and the transportable sediment size*. University of Colorado, Boulder, CO.

Bohan, J. P. (1970). *Erosion and riprap requirements at culvert and storm-drain outlets* (Research Report H-70-2). Vicksburg, MS: U.S. Army Engineer Waterways Station.

Brown, S. A., & Clyde, E. S. (1989). *Design of riprap revetment* (Hydraulic Engineering Circular No. 11). Washington, DC: Federal Highway Administration.

Fletcher, B. P., & Grace, Jr., J. L. (1972). *Practical guidance for estimating and controlling erosion at culvert outlets* (Misc. Report, H-72-2). Vicksburg, MS: U.S. Army Engineer Waterways Station.

INDOT. (2017). Hydraulics and drainage design (Chapter 203). In *Indiana design manual 2013*. Indianapolis, IN: Indiana Department of Transportation. Retrieved from https://www.in.gov/indot/design_manual/files/Ch203_2013.pdf

INDOT. (2018). *Indiana Department of Transportation 2018 standard specifications: Materials details, Section 900*. Indianapolis, IN: Indiana Department of Transportation. Retrieved from https://www.in.gov/dot/div/contracts/standards/book/sep17/sep.htm

Isbash, S. V. (1936). Construction of dams by depositing rock in running water. In *Transactions, Second Congress on Large Dams* (U.S. Government Report No. 3). Washington DC: International Congress on Large Dams.

Lagasse, P. F., Clopper, P. E., Zevenbergen, L. W., & Ruff, J. F. (2006). *Riprap design criteria, recommended specifications, and quality control* (NCHRP Report 568). Washington, DC: Transportation Research Board. Retrieved from http://onlinepubs.trb.org/onlinepubs/nchrp/nchrp_rpt_568.pdf

Lyn, D. A., & Tripathi, S. (2017). Classification analysis: Logistic regression, linear discrimination analysis, and tree classification, Chapter 6.9. In *Experimental hydraulics: Methods, instrumentation, data processing and management, Volume I: Fundamentals and methods*. London, UK: CRC Press.

Lyn, D. A., Dey, S., Saksena, S., & Merwade, V. (2018). *Assessment of HY-8 and HEC-RAS bridge models for large-span water-encapsulating structures* (Joint Transportation Research Program Publication No. FHWA/IN/JTRP-2018/14). West Lafayette, IN: Purdue University. https://doi.org/10.5703/1288284316781

Maynord, S. T., Ruff, J. F., & Abt, S. R. (1989). Riprap design. *ASCE Journal of Hydraulic Engineering*, *115*(7), 937–949. Retrieved from https://ascelibrary.org/doi/pdf/10.1061/%28ASCE%290733-9429%281989%29115%3A7%28937%29

NRCS. (2004). *Riprap design methods: Design guide MD #6*. Annapolis, MD: National Resources Conservation Service, Maryland. Retrieved from https://www.nrcs.usda.gov/Internet/FSE_DOCUMENTS/nrcs144p2_025594.pdf

Peterka, A. J. (1978). *Hydraulic design of stilling basins and energy dissipators* (U.S. Bureau of Reclamation Engineering Monograph No. 25). Washington, DC: U.S. Department of the Interior. Retrieved from https://www.usbr.gov/tsc/techreferences/hydraulics_lab/pubs/EM/EM25.pdf

Searcy, J. K. (1967). *Use of riprap for bank protection*. Washington, DC: Federal Highway Administration.

Simons, D. B., & Şentürk, F. (1992). *Sediment transport technology: Water and sediment dynamics*. Littleton, CO: Water Resources Publications.

Thompson, P. L., & Kilgore, R. T. (2006). *Hydraulic design of energy dissipators for culverts and channels* (Hydraulic Engineering Circular No. 14, Third Edition; Publication No. FHWA-NHI-06-086 HEC 14). Washington, DC: Federal Highway Administration. Retrieved from https://www.fhwa.dot.gov/engineering/hydraulics/pubs/06086/hec14.pdf

Urban Drainage and Flood Control District. (2017, September). Hydraulic structures. In *Urban Storm Drainage Criteria Manual Volume 2*. Retrieved from https://udfcd.org/wp-content/uploads/uploads/vol2%20criteria%20manual/09_Hydraulic%20Structures.pdf

U.S. Department of Agriculture, Soil Conservation Service (1989). *Loose riprap protection* (Minnesota Technical Note 3). St. Paul, MN: U.S. Department of Agriculture, Soil Conservation Service. Retrieved from https://www.nrcs.usda.gov/Internet/FSE_DOCUMENTS/nrcs142p2_022577.pdf

APPENDIX: WORKED EXAMPLES

Two examples are given to illustrate different aspects of the "hand-calculation" as well as the "spreadsheet-calculation" procedures for determining a minimum stone size for a stable apron. Here it will be assumed as before that d_{50} for INDOT revetment class, class 1, and class 2, riprap are respectively 0.58 ft, 1 ft, and 1.25 ft.

Example 1

This example takes data from an INDOT structure (70STR14, see Figure 4.11). The following data are from the HY-8 file:

discharge, Q = 137 cfs
diameter, D = 4.5 ft
tailwater depth, t_w = 1.51 ft
outlet velocity, V_{out} = 12.99 ft/s
outlet depth, y_{out} = 2.77 ft

Based solely on the outlet velocity, the INDOT design policy would choose class 2 riprap because 10 ft/s$<V_{out}<$13.5 ft/s. The proposed stone-sizing procedure is as follows:

Step 1: The procedure starts by evaluating $(d_{50})^*_I$:

$$(d_{50})^*_I = \max\left\{\frac{C_{SF,I}}{4.78}\left[\frac{V^2_{out}}{g(s-1)}\right]\max\left[1,\left(\frac{y_{out}}{t_w}\right)^{0.89}\right],0.1D\right\}$$

$$= \max\left\{\frac{1.2}{4.78}\left[\frac{(12.99\,\text{ft/s})^2}{32.2\,\text{ft/s}^2(2.65-1)}\right]\max\left[1,\left(\frac{2.83\,\text{ft}}{1.51\,\text{ft}}\right)^{0.89}\right],0.1(4.5\,\text{ft})\right\}$$

$$= \max(1.37\,\text{ft},0.45\,\text{ft}) = 1.37\,\text{ft}$$

where the safety factor, $C_{SF,I}$, has been chosen as 1.2. This result would imply a choice of an energy dissipator for a stable apron, as $(d_{50})^*_I$>1.25 ft, exceeding the assumed size of standard INDOT class 2 riprap. Thus, this result is actually *more* conservative than the INDOT design, due primarily to the relatively low-tailwater conditions.

Step 2: It is desired to explore whether a smaller riprap class would suffice, and so $(d_{50})^*_I/D$ is evaluated to check whether a smaller stone size might be possible (only if $(d_{50})^*_I/D$>0.2). It is found that $(d_{50})^*_I/D$= 1.37 ft/4.5 ft=0.30>0.2, so $(d_{50})^*_{II}$ is evaluated as

$$(d_{50})^*_{II} = \max\left\{\frac{C_{SF,II}}{6.58}\left[\frac{V^2_{out}}{g(s-1)}\right]\max\left[1.2,\left(\frac{y_{out}}{t_w}\right)^{0.86}\right],0.2D\right\}$$

$$= \max\left\{\frac{1.2}{6.58}\left[\frac{(12.99\,\text{ft/s})^2}{32.2\,\text{ft/s}^2(2.65-1)}\right]\max\left[1.2,\left(\frac{2.77\,\text{ft}}{1.51\,\text{ft}}\right)^{0.86}\right],0.2(4.5\,\text{ft})\right\}$$

$$= \max(0.98\,\text{ft},0.9\,\text{ft}) = 0.98\,\text{ft}.$$

This value is indeed smaller than that found in Step 1, and a class 1 riprap rather than a class 2 riprap might be chosen as the next larger riprap class. The value of d_{50}=0.98 ft is nevertheless very close to the value of 1 ft (the d_{50} assumed for class 1 riprap), and it should be weighed whether a class 2 riprap might not still be more appropriate.

Step 3: It may still be desired to explore whether a smaller riprap class would suffice, and so $(d_{50})^*_{II}/D$ is evaluated to check whether a smaller stone size is possible (only if $(d_{50})^*_{II}/D$>0.4). It is found that, $(d_{50})^*_{II}/D$=0.98 ft/4.5 ft=0.22<0.4, and it is concluded that a smaller stone is not possible, so the procedure is terminated, and it is not necessary to evaluate $(d_{50})^*_{III}$.

In the second procedure, the minimum adequate stone size is obtained from

$$d_{50} = \min\left[(d_{50})^*_I,(d_{50})^*_{II},(d_{50})^*_{III}\right],$$

and so all three equations need to be evaluated. The first two have already been evaluated above, so only the third is to be done:

$$(d_{50})^*_{III} = \max\left\{\frac{C_{SF,III}}{6.1}\left[\frac{V^2_{out}}{g(s-1)}\right]\max\left[1,\left(\frac{y_{out}}{t_w}\right)^{0.5}\right],0.4D\right\}$$

$$= \max\left\{\frac{1.5}{6.1}\left[\frac{(12.99\,\text{ft/s})^2}{32.2\,\text{ft/s}^2(2.65-1)}\right]\max\left[1,\left(\frac{2.77\,\text{ft}}{1.51\,\text{ft}}\right)^{0.5}\right],0.4(4.5\,\text{ft})\right\}$$

$$= \max(1.06\,\text{ft},1.8\,\text{ft}) = 1.8\,\text{ft}.$$

The final result according to the second procedure is therefore

$$d_{50} = \min[1.37\,\text{ft},0.98\,\text{ft},1.8\,\text{ft}] = 0.98\,\text{ft}.$$

which is the same as that previously obtained with the first procedure.

Example 2

This example takes data from an INDOT structure (70STR04, see Figure 4.11). The following data are from the HY-8 file:

discharge, Q = 124.3 cfs
diameter, D = 4 ft
tailwater depth, t_w = 2.58 ft
outlet velocity, V_{out} = 12.43 ft/s
outlet depth, y_{out} = 2.88 ft

Based solely on the outlet velocity, the INDOT design policy would again choose class 2 riprap as 10 ft/s$<V_{out}<$13.5 ft/s. The proposed procedure is as follows:

The "hand" calculation procedure is as follows:

Step 1: $(d_{50})^*_I$ is evaluated as

$$(d_{50})^*_I = \max\left\{\frac{C_{SF,I}}{4.78}\left[\frac{V^2_{out}}{g(s-1)}\right]\max\left[1,\left(\frac{y_{out}}{t_w}\right)^{0.89}\right],0.1D\right\}$$

$$= \max\left\{\frac{1.2}{4.78}\left[\frac{(12.43\,\text{ft/s})^2}{32.2\,\text{ft/s}^2(2.65-1)}\right]\max\left[1,\left(\frac{2.88\,\text{ft}}{2.58\,\text{ft}}\right)^{0.89}\right],0.1(4\,\text{ft})\right\}$$

$$= \max(0.81\,\text{ft},0.4\,\text{ft}) = 0.81\,\text{ft}$$

where the safety factor, $C_{SF,I}$, has been again chosen as 1.2. This result would imply a choice of the next larger INDOT standard riprap class, namely, class 1 riprap, would be adequate, and hence would improve upon the current INDOT design choice. If this choice is acceptable, then the procedure can be terminated.

Step 2: It is desired to check whether a smaller riprap class would suffice, so $(d_{50})_I^*$ is evaluated. It is found that, $(d_{50})_I^*/D = 0.81$ ft/4 ft $= 0.21 > 0.2$, and so a smaller stone is possible. $(d_{50})_{II}^*$ is evaluated as

$$(d_{50})_{II}^* = \max\left\{\frac{C_{SF,II}}{6.58}\left[\frac{V_{out}^2}{g(s-1)}\right]\max\left[1.2,\left(\frac{y_{out}}{t_w}\right)^{0.86}\right],0.2D\right\}$$

$$= \max\left\{\frac{1.2}{6.58}\left[\frac{(12.43\,\text{ft}/s)^2}{32.2\,\text{ft}/s^2(2.65-1)}\right]\max\left[1.2,\left(\frac{2.88\,\text{ft}}{2.58\,\text{ft}}\right)^{0.86}\right],0.2(4\,\text{ft})\right\}$$

$$= \max(0.64\,\text{ft},0.8\,\text{ft}) = 0.8\,\text{ft}$$

where $C_{SF,II}$ has been chosen as 1.2. The result is slightly smaller than $(d_{50})_I^*$, but in practice since the next larger riprap class remains the class 1 riprap, the ultimate choice remains the same. A smaller stone size is possible is not necessary, as $(d_{50})_{II}^*/D = 0.2 < 0.4$.

The second more spreadsheet-oriented procedure requires as in Example 1 the evaluation of all three equations, and as $(d_{50})_I^*$ and $(d_{50})_{II}^*$ has already been obtained, it remains only to evaluate $(d_{50})_{III}$ which is found as

$$(d_{50})_{III}^* = \max\left\{\frac{C_{SF,III}}{6.1}\left[\frac{V_{out}^2}{g(s-1)}\right]\max\left[1,\left(\frac{y_{out}}{t_w}\right)^{0.5}\right],0.4D\right\}$$

$$= \max\left\{\frac{1.5}{6.1}\left[\frac{(12.43\,\text{ft}/s)^2}{32.2\,\text{ft}/s^2(2.65-1)}\right]\max\left[1,\left(\frac{2.88\,\text{ft}}{2.58\,\text{ft}}\right)^{0.5}\right],0.4(4\,\text{ft})\right\}$$

$$= \max(0.76\,\text{ft},1.6\,\text{ft}) = 1.6\,\text{ft}.$$

where the safety factor, $C_{SF,III}$, has been chosen as 1.5. The minimum adequate stone size is therefore found as

$$d_{50} = \min\left[(d_{50})_I^*,(d_{50})_{II}^*,(d_{50})_{III}^*\right]$$
$$= \min[0.81\,\text{ft},0.80\,\text{ft},1.6\,\text{ft}] = 0.80\,\text{ft}$$

which again is the same result, as found by the preceding "hand"-calculation procedure.

About the Joint Transportation Research Program (JTRP)

On March 11, 1937, the Indiana Legislature passed an act which authorized the Indiana State Highway Commission to cooperate with and assist Purdue University in developing the best methods of improving and maintaining the highways of the state and the respective counties thereof. That collaborative effort was called the Joint Highway Research Project (JHRP). In 1997 the collaborative venture was renamed as the Joint Transportation Research Program (JTRP) to reflect the state and national efforts to integrate the management and operation of various transportation modes.

The first studies of JHRP were concerned with Test Road No. 1—evaluation of the weathering characteristics of stabilized materials. After World War II, the JHRP program grew substantially and was regularly producing technical reports. Over 1,600 technical reports are now available, published as part of the JHRP and subsequently JTRP collaborative venture between Purdue University and what is now the Indiana Department of Transportation.

Free online access to all reports is provided through a unique collaboration between JTRP and Purdue Libraries. These are available at http://docs.lib.purdue.edu/jtrp.

Further information about JTRP and its current research program is available at http://www.purdue.edu/jtrp.

About This Report

An open access version of this publication is available online. See the URL in the recommended citation below.

Recommended Citation

Lyn, D. A., Saksena, S., Dey, S., & Merwade, V. (2019). *A laboratory study of apron-riprap design for small-culvert outlets* (Joint Transportation Research Program Publication No. FHWA/IN/JTRP-2019/16). West Lafayette, IN: Purdue University. https://doi.org/10.5703/1288284316975